

## **Sphingosine-1-Phosphate Dependent Activation of p38 MAPK Maintains Elevated Peripheral Resistance in Heart Failure Through Increased Myogenic Vasoconstriction**

Judith Hofer, M. Ali Azam, Jeffrey T.E. Kroetsch, Howard Leong-Poi, M. Abdul Momen, Julia Voigtlaender-Bolz, Elias Q. Scherer, Anja Meissner, Steffen-Sebastian Bolz and Mansoor Husain

*Circ. Res.* 2010;107:923-933; originally published online Jul 29, 2010;

DOI: 10.1161/CIRCRESAHA.110.226464

Circulation Research is published by the American Heart Association, 7272 Greenville Avenue, Dallas, TX 75214

Copyright © 2010 American Heart Association. All rights reserved. Print ISSN: 0009-7330. Online ISSN: 1524-4571

The online version of this article, along with updated information and services, is located on the World Wide Web at:

<http://circres.ahajournals.org/cgi/content/full/107/7/923>

Data Supplement (unedited) at:

<http://circres.ahajournals.org/cgi/content/full/CIRCRESAHA.110.226464/DC1>

Subscriptions: Information about subscribing to Circulation Research is online at  
<http://circres.ahajournals.org/subscriptions/>

Permissions: Permissions & Rights Desk, Lippincott Williams & Wilkins, a division of Wolters Kluwer Health, 351 West Camden Street, Baltimore, MD 21202-2436. Phone: 410-528-4050. Fax: 410-528-8550. E-mail:  
[journalpermissions@lww.com](mailto:journalpermissions@lww.com)

Reprints: Information about reprints can be found online at  
<http://www.lww.com/reprints>

# Sphingosine-1-Phosphate–Dependent Activation of p38 MAPK Maintains Elevated Peripheral Resistance in Heart Failure Through Increased Myogenic Vasoconstriction

Judith Hoefler,\* M. Ali Azam,\* Jeffrey T.E. Kroetsch, Howard Leong-Poi, M. Abdul Momen, Julia Voightlaender-Bolz, Elias Q. Scherer, Anja Meissner, Steffen-Sebastian Bolz,† Mansoor Husain†

**Rationale:** Mechanisms underlying vasomotor abnormalities and increased peripheral resistance exacerbating heart failure (HF) are poorly understood.

**Objective:** To explore the role and molecular basis of myogenic responses in HF.

**Methods and Results:** 10 weeks old C57Bl6 mice underwent experimental myocardial infarction (MI) or sham surgery. At 1 to 12 weeks postoperative, mice underwent hemodynamic studies, mesenteric, cerebral, and cremaster artery perfusion myography and Western blot. Organ weights and hemodynamics confirmed HF and increased peripheral resistance after MI. Myogenic responses, ie, pressure-induced vasoconstriction, were increased as early as 1 week after MI and remained elevated. Vasoconstrictor responses to phenylephrine were decreased 1 week after MI, but not at 2 to 6 weeks after MI, whereas those to endothelin (ET)-1 and sphingosine-1-phosphate (S1P) were increased at all time points after MI. An antagonist (JTE-013) for the most abundant S1P receptor detected in mesenteric arteries (S1P<sub>2</sub>R) abolished the enhanced myogenic responses of HF, with significantly less effect on controls. Mice with genetic absence of sphingosine-kinases or S1P<sub>2</sub>R (*Sphk1*<sup>-/-</sup>; *Sphk1*<sup>-/-</sup>/*Sphk2*<sup>+/-</sup>; *S1P<sub>2</sub>R*<sup>-/-</sup>) did not manifest enhanced myogenic responses after MI. Mesenteric arteries from HF mice exhibited increased phosphorylation of myosin light chain, with deactivation of its phosphatase (MLCP). Among known S1P-responsive regulators of MLCP, GTP-Rho levels were unexpectedly reduced in HF, whereas levels of activated p38 MAPK and ERK1/2 (extracellular signal-regulated kinase 1/2) were increased. Inhibiting p38 MAPK abolished the myogenic responses of animals with HF, with little effect on controls.

**Conclusions:** Rho-independent p38 MAPK-mediated deactivation of MLCP underlies S1P/S1P<sub>2</sub>R-regulated increases in myogenic vasoconstriction observed in HF. Therapeutic targeting of these findings in HF models deserves study. (*Circ Res.* 2010;107:923-933.)

**Key Words:** myogenic response ■ heart failure ■ sphingosine-1-phosphate ■ mitogen-activated protein kinase

Heart failure (HF) is a progressive condition that affects more than 2% of the population and accounts for ≈\$28 billion in health care costs in the United States.<sup>1</sup> The prevalence of HF is increasing worldwide, and given its adverse impacts on the quality and longevity of life,<sup>1</sup> the burdens imposed by HF are enormous. Irrespective of etiology, HF presents as a clinical syndrome of reduced cardiac output and or elevated cardiac filling pressures.<sup>2–4</sup> In the former, cardiac-renal-hormonal axes and sympathetic neural reflexes are activated in an attempt to maintain sufficient

mean arterial pressure (MAP) for vital organ perfusion.<sup>4</sup> This is achieved through increased salt and water retention<sup>4</sup> (ultimately worsening the deleterious volume overload of HF), and through an increase in peripheral resistance (PR).<sup>5</sup> Although increased PR may support MAP in certain circumstances, chronic elevations in PR contribute to a pressure afterload that further limits cardiac output in HF,<sup>3</sup> and drives adverse cardiac remodeling.<sup>3</sup> Such “vicious cycles” are believed to play a key role in the progressive nature of HF, and many advances in its management have been aimed at

Original received August 5, 2009; resubmission received June 18, 2010; revised resubmission received July 19, 2010; accepted July 20, 2010. In June 2010, the average time from submission to first decision for all original research papers submitted to *Circulation Research* was 14.5 days.

From the Institute of Medical Science (J.H., M.H.), Heart and Stroke Richard Lewar Centre of Excellence (J.H., M.A.A., J.T.E.K., H.L.-P., J.V.-B., A.M., S.-S.B., M.H.), and Departments of Physiology (J.T.E.K., A.M., S.-S.B., M.H.) and Medicine (M.H.), University of Toronto, Canada; Division of Cell and Molecular Biology (J.H., M.A.A., M.A.M., M.H.), Toronto General Hospital Research Institute, Canada; Terrence Donnelley Research Centre (H.L.-P., J.V.-B.), St Michael's Hospital, Toronto, Canada; and Klinikum Rechts der Isar (E.Q.S.), Technische Universität München, Germany.

\*Both authors contributed equally to this work as first authors.

†Both authors contributed equally to this work as senior authors.

Correspondence to Mansoor Husain, Toronto General Hospital Research Institute, TMDT-3-909, 200 Elizabeth St, Toronto, ON M5G-2C4, Canada. E-mail mansoor.husain@utoronto.ca

© 2010 American Heart Association, Inc.

*Circulation Research* is available at <http://circres.ahajournals.org>

DOI: 10.1161/CIRCRESAHA.110.226464

Non-standard Abbreviations and Acronyms	
<b>ACh</b>	acetylcholine
<b>ERK</b>	extracellular signal-regulated kinase
<b>ET-1</b>	endothelin-1
<b>HF</b>	heart failure
<b>ILK</b>	integrin-linked kinase
<b>LAD</b>	left anterior descending
<b>MAP</b>	mean arterial pressure
<b>MAPK</b>	mitogen-activated protein kinase
<b>MI</b>	myocardial infarction
<b>MLC</b>	myosin light chain
<b>MLCK</b>	myosin light chain kinase
<b>MLCP</b>	myosin light chain phosphatase
<b>PE</b>	phenylephrine
<b>PR</b>	peripheral resistance
<b>RAS</b>	renin-angiotensin system
<b>ROS</b>	reactive oxygen species
<b>S1P</b>	sphingosine-1-phosphate
<b>SNP</b>	sodium nitroprusside
<b>VSMC</b>	vascular smooth muscle cell
<b>VTI</b>	velocity-time integral
<b>ZIPK</b>	zipper interacting protein kinase

mitigating this pathophysiology. In general, increased PR in HF is thought to be conveyed by neurohumoral activation, including the sympathetic nervous system,<sup>6</sup> the renin-angiotensin system (RAS),<sup>4</sup> and local mechanisms such as the myogenic response.<sup>7</sup> Our present purpose was to investigate the molecular mechanisms that underlie the latter, ie, myogenic elevations of PR in HF, to identify potentially novel therapeutic targets.

Indeed, growing evidence suggests that long-term elevations in PR depend more on “local” vascular mechanisms than systemic factors such as the sympathetic activation of orthostasis.<sup>5</sup> Moreover, reasons why chronic maintenance of high PR in HF by systemic sympathetic (ie,  $\alpha_1$ -adrenergic) enhancement of peripheral vasoconstriction<sup>2,8</sup> is disadvantageous include: (1) increased sympathetic output compromises a failing myocardium (via tachycardia, arrhythmia, cytotoxicity<sup>9</sup>); and (2) catecholamine potency diminishes because of adrenergic receptor desensitization.<sup>10–12</sup> We thus posited that distinct local mechanisms would participate in chronic elevations in PR observed in HF. Supporting this premise, the maintenance of peripheral vascular tone largely depends on “myogenic” mechanisms intrinsic to vascular smooth muscle cells (VSMCs).<sup>13</sup> On a local level, myogenic mechanisms serve to adapt vascular tone to changes in transmural pressure. Systemically, myogenic vasoconstriction can amplify vasopressor responses by positive feedback on systemic blood pressure. This has been elegantly demonstrated by Metting et al, who showed that 74% of the phenylephrine (PE)-mediated increase in MAP relied on a myogenic mechanism.<sup>14</sup> Accordingly, we hypothesized that an increase in myogenic tone would underlie the long-term elevation of PR observed in HF. Although increased myogenic responses

have been found in rats with HF,<sup>7</sup> a mechanistic explanation for this finding remained elusive. Based on our understanding of myogenic tone,<sup>15–21</sup> we sought to more fully explore the molecular pathways temporally activated in the resistance mesenteric arteries of mice with HF.

Our results reveal a heretofore unrecognized importance of S1P signaling in the development of increased PR in a mouse post-MI model of HF. In this model, we describe the rapid emergence of enhanced myogenic response, with its near complete dependence on the vascular signaling molecule S1P, the S1P<sub>2</sub> receptor (S1P<sub>2</sub>R) found on mesenteric arteries, and an unexpectedly Rho-independent inactivation of myosin light chain phosphatase (MLCP). Our finding of enhanced p38 MAPK and extracellular signal-regulated kinase (ERK)1/2 activation and the susceptibility of increased myogenic response of HF animals to a p38 MAPK inhibitor suggest novel therapeutic targets.

## Methods

An expanded Methods section is available in the Online Data Supplement at <http://circres.ahajournals.org>.

## Reagents

Drugs, chemicals and antibodies were purchased from Sigma-Aldrich unless otherwise indicated, including L-phenylephrine (PE), acetylcholine chloride (ACh), sodium-nitroprusside (SNP), sphingosine-1-phosphate (S1P), D-erythro (Biomol International), the S1P<sub>2</sub>R antagonist JTE-013 (Trocris Bioscience), and the p38 MAPK inhibitor SB203580 (Cayman Chemical). Glutathione S-transferase-Rhotekin was prepared as described.<sup>22</sup> Additional reagents are described in the Online Data Supplement.

## Animals

Experiments were conducted in accordance with protocols approved by our institutional Animal Care Committee. Wild-type male C57BL/6 mice (Charles River) and knockout strains were housed under 12 hour:12 hour light-dark cycles with normal chow and water ad libitum. Mice at 10 weeks of age underwent surgery to induce a myocardial infarction (MI) or a sham procedure, as described.<sup>23</sup> Mice were euthanized at prespecified time points 1 to 12 weeks postoperative.

## Hemodynamics and Echocardiography

Aortic and left ventricular pressure measurements were made as described.<sup>24</sup> Transthoracic echocardiography was conducted under identical anesthesia using a 30 MHz mechanical sector transducer (Vevo 770, Visual Sonics). Measurements and calculations used are described in the Online Data Supplement.

## Perfusion Myography

Mice were euthanized and either mesenteric, posterior cerebral or cremaster muscle arteries were rapidly dissected and prepared for perfusion myography as detailed in the Online Data Supplement. Viability of the vessel preparations was assessed using 3  $\mu$ mol/L PE; endothelial viability was subsequently assessed with 3  $\mu$ mol/L ACh. Concentration-dependent vasoconstriction relationships for PE (1 nmol/L–30  $\mu$ mol/L), ET-1 (0.01 nmol/L–10 nmol/L) and S1P (1 nmol/L–10  $\mu$ mol/L) were determined. Concentration-dependent vasodilation to ACh (1 nmol/L–30  $\mu$ mol/L) and SNP (1 nmol/L–30  $\mu$ mol/L) were determined in arteries precontracted with 3  $\mu$ mol/L PE. In some experiments, vessels were treated with S1P<sub>2</sub>R antagonist JTE-013 (1  $\mu$ m; 30 minutes) following dose-response assessments and then retested. At the completion of each experiment, a Ca<sup>2+</sup>-free buffer was used to record passive diameter (dia<sub>passive</sub>). Vessel tone was calculated as: (dia<sub>passive</sub> – dia<sub>response</sub>)/dia<sub>passive</sub>, where dia<sub>response</sub> is the diameter at a given drug concentration.

**Table. Mouse Characteristics and Cardiac Function in Sham and HF Mice**

Parameter	1 Week		2 Weeks		4 Weeks		6 Weeks		12 Weeks	
	Sham	HF	Sham	HF	Sham	HF	Sham	HF	Sham	HF
Infarct size (%)		33.1±0.6*		32.3±1.3*		35.4±1.1*		33.1±1.6*		34.1±0.3*
Body weight (g)	25.1±0.1	28.3±0.3*	25.2±0.1	26.9±0.2*	26.9±0.3	29.9±0.7*	26.9±0.51	30.0±0.7*	26.9±0.5	30.0±0.7*
Heart weight (g)	0.19±0.01	0.25±0.02*	0.19±0.02	0.28±0.01*	0.14±0.01	0.26±0.01*	0.17±0.01	0.28±0.01*	0.15±0.01	0.20±0.01*
Heart/body (mg/g)	7.4±0.3	9.0±0.4*	7.5±0.2	10.3±0.2*	5.3±0.3	8.7±0.6*	6.4±0.4	10.0±0.2*	5.59±0.5	9.93±0.2*
Lung weight (mg)	210±1	254±2*	202±1	300±1*	187±2	283±3	190±6	287±2*	180±6	281±4*
Liver weight (g)	1.30±0.05	1.50±0.05*	1.30±0.01	1.50±0.01*	1.30±0.01	1.60±0.03*	1.30±0.01	1.60±0.06*	1.40±0.04	1.60±0.10*
Heart rate (bpm)	404±30	419±28					398±18	417±19		
LVEF (%)	60±7	34±3*					62±4*	23±4*		
Stroke volume (mL)	138±2	85±2*					130±4*	70±7*		
LVESP (mm Hg)	112±2	98±1*					114±0.6	98±2.0*		
LVEDP (mm Hg)	5.7±0.5	18.3±2*					2.0±0.6	7.0±2.8*		

Data are mean±SE. \* $P<0.05$  compared to Sham.

To assess the myogenic response, transmural pressure was increased in 20 mm Hg steps from 20 to 120 mm Hg. Vessel diameter (active) was measured at each pressure step once a steady state was reached (5 to 10 minutes). In some experiments, vessels were treated with JTE-013 (1  $\mu\text{mol/L}$ ; 30 minutes) or SB203580 (5  $\mu\text{mol/L}$ ; 30 minutes) following the myogenic response assessment and retested. At completion, passive diameter ( $\text{dia}_{\text{passive}}$ ) was recorded for each pressure step. Myogenic tone at each step was calculated as:  $(\text{dia}_{\text{passive}} - \text{dia}_{\text{active}}) / \text{dia}_{\text{passive}}$ . Myogenic index, a measure of the strength of the myogenic response at each pressure step, was calculated as previously described.<sup>25</sup>

### Histology, Western Blot, VSMC Isolation, and RT-PCR

These details are provided in the Online Data Supplement.

### Statistical Analysis

All data are expressed as means±SE; n values represent the number of mice or arteries (although no more than 1 artery segment per mouse was used for the same protocol). All data were analyzed with a Student's unpaired *t* test, with the exception of myogenic responses, which were analyzed with repeated measures ANOVA, followed by *t*-tests with Bonferonni correction. PCR and Western blot data were analyzed as described above. For a comparison between control and treatment groups the resulting relative expression ratios were directly compared using a Student's unpaired *t* test. Differences were considered significant at  $P<0.05$ .

## Results

### HF Develops in Mice After MI

The left anterior descending (LAD) ligation model generated a reproducible infarct size ( $33.6\pm 1.1\%$ ,  $n=40$ ) with compelling evidence of HF never observed in sham-operated controls (Table). Compared to sham, post-MI animals showed evidence of fluid retention and organ congestion as manifest by increased body, heart, lung, and liver weights and an increase in the heart:body weight ratio at 1, 2, 4, 6, and 12 weeks after MI. At 1 and 6 weeks after MI, echocardiography revealed left ventricular dilatation (1 week:  $5.1\pm 0.6$  mm,  $n=4$ , versus  $3.8\pm 0.3$  mm,  $n=6$ ; 6 weeks:  $6.5\pm 0.1$  versus  $4.5\pm 0.1$  mm,  $n=5$  for both;  $P<0.001$  for both), with reduced fractional shortening (1 week:  $12\pm 1$  versus  $26\pm 2$ ; 6 weeks:  $8\pm 1$  versus  $28\pm 2$ ; %,  $P<0.0001$  for both) and ejection fraction (Table). Other signs of cardiac contractile dysfunction

included diminished stroke volume and reduced cardiac output (Figure 1A; Online Figure I, A) developed without differences in heart rate (HR) between HF and sham groups (Table). A significant increase in calculated PR was also found in the HF group (Figure 1B; Online Figure I, B), suggesting partial compensation for their reduced MAP (Figure 1C; Online Figure I, C).

### Resistance Artery Structure Is Not Altered in Mice With HF

To examine whether structural changes in resistance arteries accompany observed increases in PR, media mass and collagen content were assessed in histological sections of second order mesenteric arteries from mice with HF as compared to sham controls. At 6 weeks after surgery, neither parameter was different between the two groups, with maximal passive mesenteric artery diameters further suggesting an absence of structural remodeling (Online Figure II).

### Resistance Artery Functions Are Specifically Altered in Mice With HF

Mesenteric arteries from HF and sham were subjected to a series of vasomotor studies to determine both the nature and extent of functional differences. Concentration-dependent vasoconstriction to the  $\alpha_1$ -agonist PE tested at 1 week after MI showed reduced responsiveness in mesenteric arteries from animals with HF versus sham controls (Figure 2A). In contrast, concentration-dependent vasoconstriction to PE at all later time points did not differ between HF and sham mice (Figure 2B; data not shown for 2, 4, 12 weeks). Indeed, a PE dose (3  $\mu\text{mol/L}$ ) induced near identical levels of vessel precontraction at 6 weeks postoperative (HF:  $71\pm 2.5$ ; sham:  $70.6\pm 2.6$ ; % passive diameter at 60 mm Hg;  $P=\text{NS}$ ), following which applications of ACh and SNP were used to assess endothelium-dependent and endothelium-independent vasodilatory responses respectively. Neither ACh nor SNP dose-response relationships differed between HF versus sham groups (Online Figure III: ACh,  $\text{EC}_{50}$   $0.8\pm 0.3$  versus  $1.2\pm 0.3$   $\mu\text{mol/L}$ ; SNP  $\text{EC}_{50}$   $0.6\pm 0.1$  versus  $0.4\pm 0.1$   $\mu\text{mol/L}$ ;  $n=6$ ,  $P=\text{NS}$  for both).

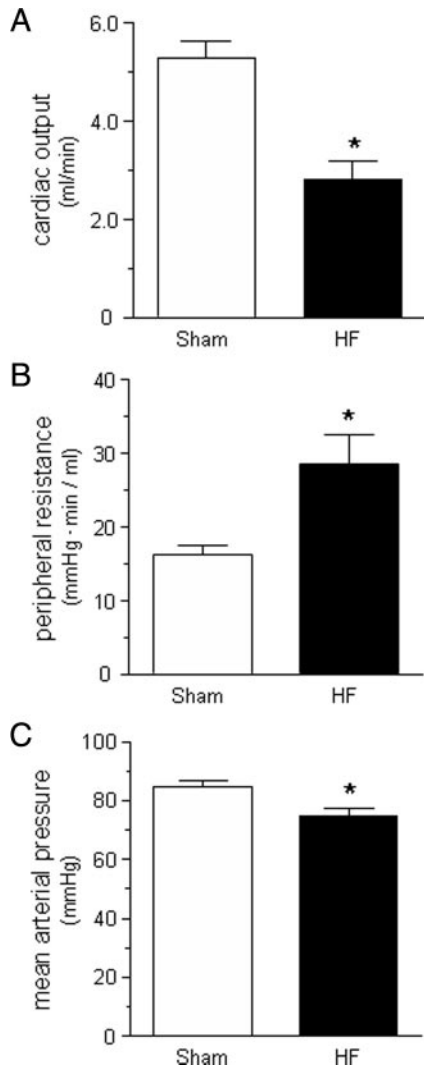


**Figure 1. Hemodynamic parameters in HF mice.** Measurements of cardiac output (CO) (A), PR (B), and MAP (C) in sham (n=5) and HF (n=5) mice at 6 weeks after surgery. MAP and cardiac output were reduced in HF vs sham. PR was increased in HF vs sham. Data are means±SE. \*P<0.05.

In contrast to these results, vasoconstrictor responses to increasing concentrations of ET-1 (0.01 to 10 nmol/L) were greater in mesenteric arteries from animals with HF versus sham (Online Figure IV, A). To examine if this was a function of enhanced Ca<sup>2+</sup> sensitivity of the contractile

apparatus, mesenteric arteries were exposed to increasing concentrations of extracellular Ca<sup>2+</sup> (0.25 to 3.0 mmol/L) in perfusion buffers containing a depolarizing level of K<sup>+</sup> (125 mmol/L). Under these conditions, no difference was found in Ca<sup>2+</sup> sensitivity (data not shown). Together, these studies suggested that the increase in ET-1 sensitivity that accompanies the development of HF in mice was a ligand/receptor-specific effect of enhanced pharmacomechanical (but not electromechanical) coupling.

**Increased Myogenic Responses in HF Becomes More S1P<sub>2</sub>R-Dependent Over Time**

We next assessed whether pressure-induced (ie, myogenic) vasoconstriction was increased in mice with HF. Myogenic responses to perfusion pressures 20 to 120 mm Hg were markedly increased in mesenteric arteries from HF versus sham-operated mice (Figure 3A through 3D), including significant increases in the “resting tone” (defined as the myogenic tone at perfusion pressure 60 mm Hg; P<0.05 for all time-points; Figure 3) and the “myogenic index” (Online Figure V). Having recently shown that the phospholipid mediator S1P is an integral component of the pathway that regulates the myogenic response in hamster,<sup>17</sup> we sought to explore a similar role for S1P in mice with HF. In this regard, the S1P<sub>2</sub>R-selective inhibitor JTE-013 reduced myogenic response in arteries from sham mice by only modest levels (28.0±4.5% at 120 mm Hg) at all time points tested. Although mesenteric arteries from HF mice showed a similarly limited contribution of S1P to the myogenic response at 1 week after MI (ie, JTE-013-induced inhibition of myogenic response was 30.8% at 120 mm Hg; Figure 3A), this proportion substantively increased at later time points (2, 4, and 6 weeks postoperative: 88.5%, 88.1%, and 84.1%; Figure 3B through 3D). This result indicated that the enhanced myogenic response of mice with HF becomes more S1P<sub>2</sub>R-dependent more than time. Importantly, JTE-013 had no effect on ET-1-induced vasoconstriction (Online Figure IV, B).

To ascertain whether the increased myogenic responses of mesenteric arteries observed in HF was a generalized effect, perfusion myography was also conducted on posterior cerebral arteries (data not shown) and cremaster skeletal muscle arterioles (Figure 4). These studies confirmed increased myogenic responses in each vascular bed examined in HF, and thus a generalized systemic effect of HF consistent with hemodynamic evidence of increased PR (Figure 1B; Online Figure I, B).

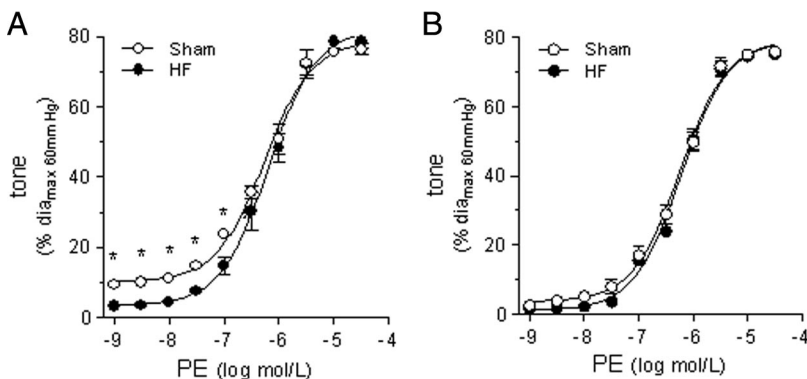


**Figure 2. Vasomotor response to PE 1 week and 6 weeks after MI.** Concentration-dependent vasoconstriction to PE was greater in mesenteric arteries (MA) isolated from sham vs HF mice at 1 week (P=0.05; 2-way ANOVA) (A) but not 6 weeks after MI (P=NS) (B). For all groups, n=6; Data are means±SE. \*P<0.05 by post hoc analysis.

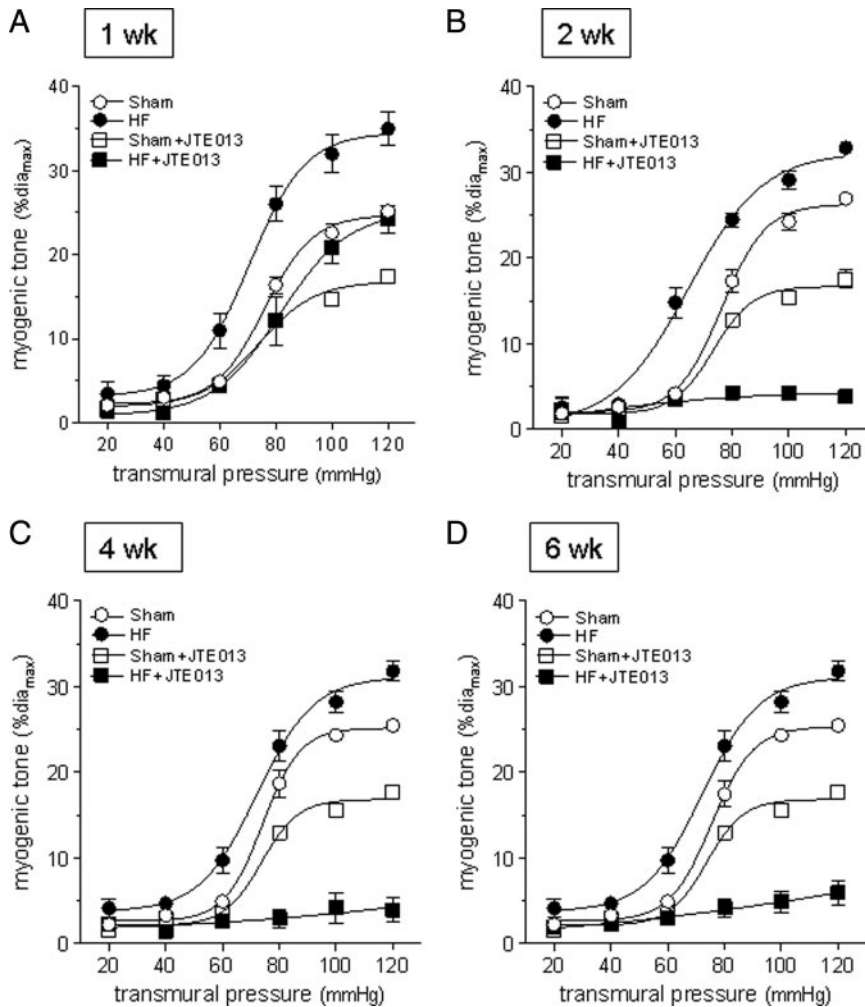


**Figure 3. Myogenic tone in isolated mesenteric arteries from HF mice.** Myogenic responses (MR) were augmented in mesenteric arteries (MA) isolated from HF mice at 1 (A), 2 (B), 4 (C), and 6 (D) weeks after MI, compared to sham mice;  $P < 0.05$  by 2-way ANOVA for all time points. Blockade of the S1P<sub>2</sub>R (JTE-013, 1  $\mu\text{mol/L}$ ) reduced MR in MA from both sham and HF mice at 1 (A), 2 (B), 4 (C), and 6 (D) weeks post-operative;  $P < 0.05$  at 1 week and  $P < 0.001$  by 2-way ANOVA at all other time points. At 1 week (A), the JTE-013-mediated reduction in MR was near equal for HF and sham. At all other time points (B through D), JTE-013 virtually abolished MR in MA from HF mice. For all groups,  $n \geq 6$ . Data are means  $\pm$  SE.

### Myogenic Responses in Mesenteric Arteries From Mice Without HF Only Partially Depend on S1P/S1P<sub>2</sub>R

Having previously reported a key role for S1P and S1P<sub>2</sub>R in regulating the myogenic response in hamster,<sup>17</sup> we had expected the S1P<sub>2</sub>R antagonist JTE-013 to have significant effects on the myogenic response of mesenteric arteries from both HF and sham mice. We were thus surprised to observe the limited effect of S1P<sub>2</sub>R blockade on myogenic responses in mesenteric arteries from sham mice (Figure 3), and sought additional evidence to support this finding. We examined myogenic responses in mesenteric arteries isolated from mice with genetic deletion of sphingosine kinase-1 (*Sphk1*<sup>-/-</sup>),<sup>24</sup> the predominant source of pressure-induced S1P synthesis in hamster.<sup>17</sup> The myogenic response elicited by a pressure step from 45 to 110 mm Hg in mesenteric arteries from *Sphk1*<sup>-/-</sup> and wild-type littermates were virtually identical ( $109 \pm 8\%$ ,  $n = 5$  versus  $102 \pm 9\%$ ,  $n = 5$ ,  $P = \text{NS}$ ), suggesting that genetic absence of *Sphk1*<sup>-/-</sup> can be completely compensated for, and supporting our observation that S1P/S1P<sub>2</sub>R may only partially mediate myogenic responses in mesenteric arteries isolated from animals without HF (ie, in sham- or unoperated mice, Figure 3). Consistent with previous data from hamster,<sup>17</sup> myogenic responses of cremaster and cerebral arteries

were fully mediated by S1P (ie, abrogated by JTE-013, Figure 4A and data not shown) and enhanced in arteries from HF mice.

### Effects of S1P on Mesenteric Arteries From Animals With HF

To further explore the role of S1P/S1P<sub>2</sub>R in myogenic responses in HF, the S1P dose-response relationship was examined in HF and sham mice. These studies revealed greater vasoconstriction at every S1P concentration tested (1 nmol/L–10  $\mu\text{mol/L}$ ) in the HF group (Figure 5). With the exception of the highest S1P concentration tested (10  $\mu\text{mol/L}$ ), the enhanced vasoconstriction to S1P observed in mice with HF was entirely attributable to S1P<sub>2</sub>R activation, as gauged by the effects of JTE-013 (Figure 5B). Consistent with this result, we were unable to detect mRNA encoding any S1P receptor other than S1P<sub>2</sub>R in either whole mesenteric arteries or VSMCs isolated from mesenteric arteries (Online Figure VI).

### HF in *Sphk1*<sup>-/-</sup>, *Sphk1*<sup>-/-</sup>/*Sphk2*<sup>+/-</sup>, and S1P<sub>2</sub>R<sup>-/-</sup> Mice Was Not Associated With Enhanced Myogenic Response

To further investigate the importance of the S1P/S1P<sub>2</sub>R signaling pathway in the regulation of myogenic response in

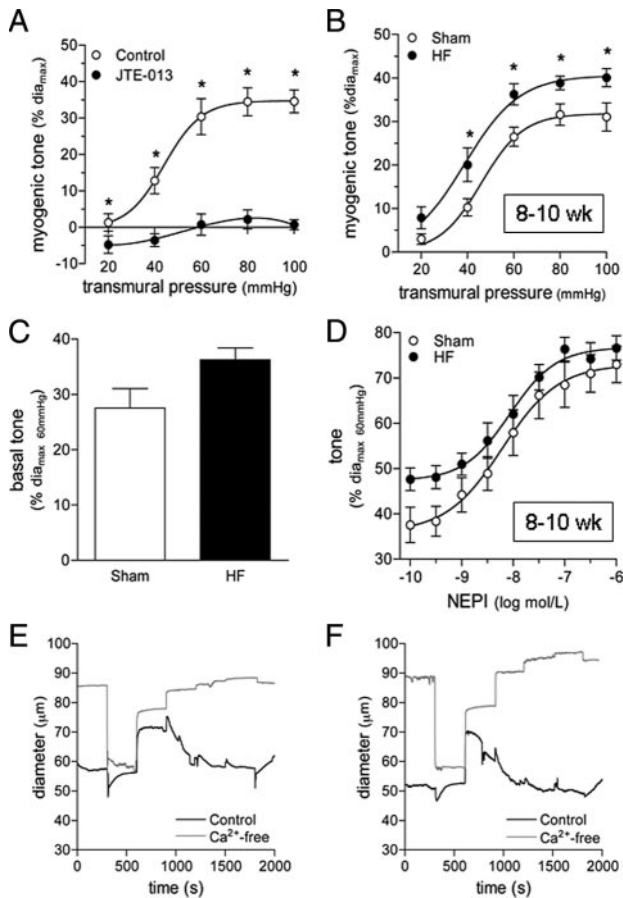


**Figure 4. Perfusion myography of cremaster muscle arteries.** In cremaster arteries from normal C57/BL6 mice (A), myogenic tone was abrogated following incubation with the S1P2R antagonist JTE-013 (1  $\mu\text{mol/L}$ ;  $n=4$ ;  $*P<0.05$ ). Cremaster arteries from HF mice 8 to 10 weeks postoperative revealed augmented myogenic responses to elevations in transmural pressure ( $n=7$  each;  $*P<0.05$ ) (B), a trend to increased basal tone (60 mm Hg;  $n=7$  each;  $P=0.05$ ) (C), and no difference in vasoconstrictor responses to norepinephrine (NEPI: 0.1 nmol/L to 1  $\mu\text{mol/L}$ ;  $n=7$  each;  $P=NS$ ) (D). Data are means  $\pm$  SE. Representative myogenic responses in cremaster arteries from sham (E) and HF (F) mice. Control and  $\text{Ca}^{2+}$ -free indicate active and passive responses, respectively.

HF, genetic mutants of the S1P signaling pathway were also subjected to experimental MI. Unlike the wild-type, none of the mutants tested manifest enhanced myogenic response at 4 weeks after MI (Online Figure VII). Having said this, *Sphk1*<sup>-/-</sup>/*Sphk2*<sup>+/-</sup> mice were still able to increase PR at this time-point in HF as compared to sham-operated controls (Online Figure VIII).

### MLCP Is Inactivated in Mice With HF

To determine molecular mechanisms underlying our findings, we first measured levels of activated (ie, Ser19 phosphorylated) myosin light chain (MLC) in mesenteric arteries from animals 6 weeks after MI or sham surgery. As expected, Ser19 phosphorylation of MLC was  $28.0 \pm 5.9\%$  greater in mesenteric arteries from HF versus sham (Figure 6A,  $P=0.04$ ), a result consistent with enhanced activity of MLC-specific kinase (MLCK) or diminished activity of MLC-specific phosphatase (MLCP) in HF.

As the balance between MLCK and MLCP activities determines the contractile status of VSMCs,<sup>26</sup> we next examined levels of active and inactive MYPT1, the regulatory subunit of MLCP. Relative amounts of inactive MLCP (ie, Thr850-phosphorylated MYPT1) were  $2.33 \pm 0.15$  fold greater in mesenteric arteries from HF than sham (Figure 6B). This result suggested that inactivation of MLCP plays a major role in the ligand/receptor-specific vasoconstrictor responses and increased myogenic response and PR documented in HF.

We next studied which of the several known upstream regulators of MYPT1 may be mediating the effects observed in HF. First, it is known that Rho-kinase phosphorylates MYPT1, inactivating MLCP and enhancing vasoconstrictor responses, including  $\text{Ca}^{2+}$  sensitivity in VSMCs.<sup>27</sup> As Rho cycles between GDP (inactive) and GTP (active) forms, we directly measured levels of GTP-Rho in mesenteric arteries with an established pull-down assay using GST-Rhotekin.<sup>27</sup> To our surprise, we found that levels of GTP-Rho were markedly reduced in mesenteric arteries from mice with HF (Figure 6C). This result strongly suggested that the inactivating phosphorylation of MYPT1 seen in HF was not mediated by GTP-Rho/Rho-kinase.

### Mesenteric Arteries of Mice With HF Manifest Increased Activation of p38 MAPK and ERK1/2

In VSMCs, a specific MLCP inhibitor known as CPI-17 has been described.<sup>28</sup> Both Rho-kinase and protein kinase C are known to Thr38-phosphorylate CPI-17, which dramatically increases its ability to inhibit MLCP.<sup>28</sup> Additional upstream negative regulators of MYPT1, including zipper interacting protein kinase (ZIPK)<sup>29</sup> and integrin-linked kinase (ILK)<sup>30</sup> were also examined in mesenteric arteries from HF and sham mice. Western blots revealed a nonsignificant increase in Thr38-phosphorylation of CPI-17 (CPI-17:  $1.33 \pm 0.15$  versus  $1.00 \pm 0.11$ ,  $n=8$ ,  $P=NS$ ) and no significant differences in expression levels of ZIPK and ILK (data not shown). Having said this, we have not directly measured activity levels of the latter kinases.

To examine other upstream regulators of MLCP, we next assayed known protein kinase C-dependent mitogen-activated protein kinases (MAPKs) known to inhibit MYPT1 of gut smooth muscle via ZIPK and ILK, namely p38 MAPK and ERK1/2.<sup>31–33</sup> Western blots revealed that activating Thr202/Tyr204-phosphorylation of ERK1/2 was modestly increased in mesenteric arteries of mice with HF as compared to sham controls (Online Figure IX, A). This change was dwarfed by the large increase in levels of phosphorylated (ie, active) p38 MAPK observed in mesenteric arteries from animals with HF versus sham ( $2.21 \pm 0.24$  versus  $1.00 \pm 0.31$ ,  $n=4$ ,  $P=0.004$ ) (Figure 6D).

To assess whether p38 MAPK and ERK1/2 in intact mesenteric arteries are subject to activation by S1P, Western blots were performed on protein extracts from mesenteric arteries of wild-type uninjured mice exposed to S1P (2  $\mu\text{mol/L}$  x 10 minutes). Although levels of phospho-ERK1/2 were increased (Online Figure IX, B), no activation of p38 MAPK was observed following this acute treatment protocol (data not shown). However, in the chronic HF

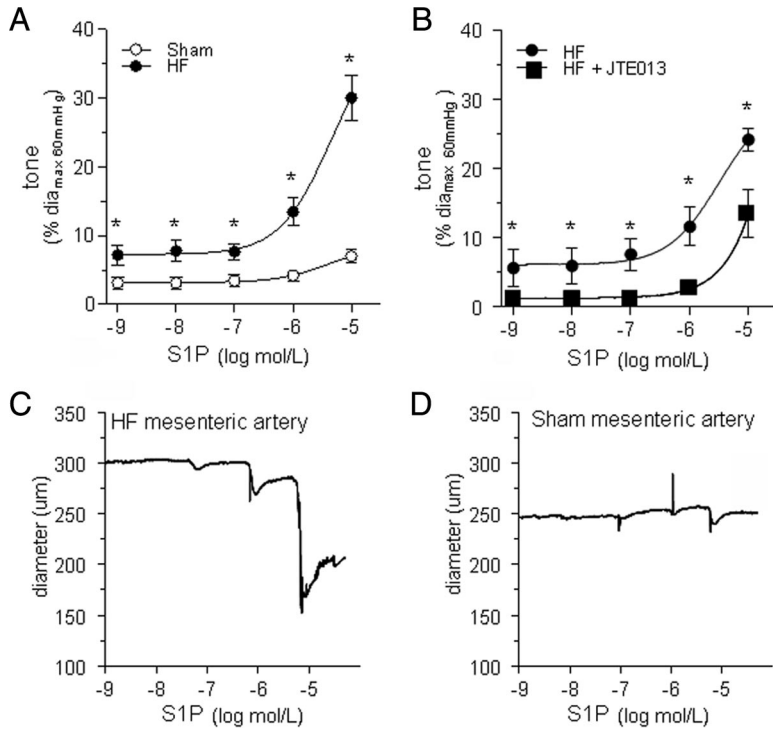


**Figure 5. Vasomotor responses to S1P.** **A**, Concentration-dependent vasoconstriction to S1P was enhanced in mesenteric arteries (MA) isolated from HF mice vs sham;  $P < 0.0001$  by 2-way ANOVA. **B**, The S1P2R-selective antagonist JTE013 (1  $\mu\text{mol/L}$ ) virtually abolished S1P-mediated vasoconstriction in MA from HF mice;  $P < 0.05$  by 2-way ANOVA. Data are means  $\pm$  SE. \* $P < 0.05$  by post hoc analysis. **C** and **D**, Representative tracings of concentration-dependent vasoconstrictions to S1P in a single vessel from a HF (**C**) and sham (**D**) mouse.

setting, a p38 MAPK inhibitor completely abolished the increased myogenic response of mesenteric arteries, having significantly less effect on the myogenic response of mesenteric arteries isolated from sham animals (Figure 7).

**Discussion**

Our ex vivo studies of isolated mesenteric arteries from mice with HF and increased PR have revealed (1) enhanced myogenic responses and (2) augmented vasoconstrictor re-

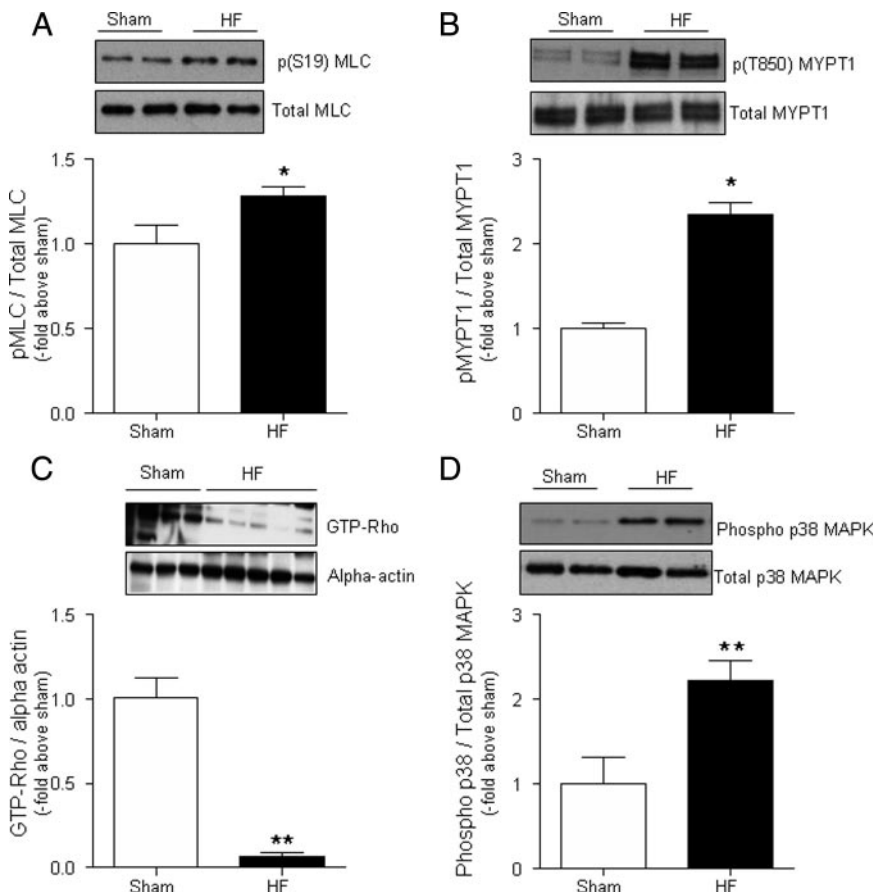


**Figure 6. MLC, MYPT1, GTP-Rho, and p38 MAPK levels in HF and sham mice.** Western blots of mesenteric artery (MA) protein extracts from mice 6 weeks after MI (HF) or sham were probed for MLC and Ser19-phosphorylated MLC (**A**), MYPT1 and Thr850-phosphorylated MYPT1 (**B**), GTP-Rho (**C**), and p38 MAPK and Thr180/Tyr182-phosphorylated p38 MAPK (**D**). Representative blots and densitometric quantifications (means  $\pm$  SE,  $n = 8$  to 9 for A, B, and D;  $n = 3$  to 5 for C) are shown. \* $P < 0.05$ ; \*\* $P < 0.01$ .

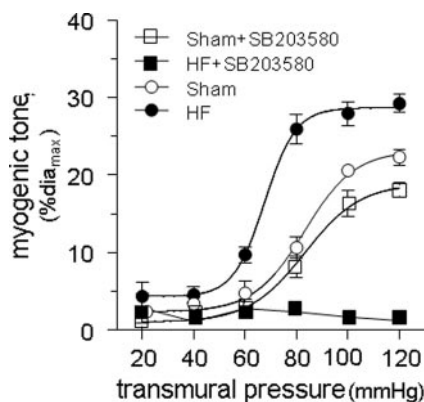


**Figure 7. Myogenic tone in mesenteric arteries before and after p38 MAPK inhibition.** Myogenic responses (MR) were augmented in mesenteric arteries (MA) isolated from HF mice vs sham at 6 weeks postoperative;  $P < 0.01$  by 2-way ANOVA. Blockade of p38 MAPK activation with SB203580 (5  $\mu\text{mol/L}$ ) did not cause a significant reduction of MR in MA from sham;  $P = \text{NS}$  (0.25 by 2-way ANOVA) but completely abolished myogenic response in mesenteric arteries from HF mice.  $P < 0.0001$  by 2-way ANOVA. For all groups,  $n = 4$ . Data are means  $\pm$  SE.

sponses to specific ligands, without structural vascular remodeling or a generalized increase in  $\text{Ca}^{2+}$  sensitivity of the contractile apparatus.<sup>19</sup> We also discovered (3) that although S1P and S1P<sub>2</sub>R signaling plays a minor role in regulating the myogenic response of mesenteric arteries from control animals, or from those animals in the early stages of HF (<2 weeks), S1P and S1P<sub>2</sub>R play a dominant role in the myogenic responses of normal mouse cremaster arterioles and in the pathophysiology of enhanced myogenic responses of all vascular beds examined as HF progresses over time. Indeed, in the later stages examined (2 to 12 weeks; see Figure 3), myogenic responses of mesenteric arteries became almost entirely dependent on S1P/S1P<sub>2</sub>R signaling. Importantly, increased myogenic tone was a generalized response of all systemic arteries examined, as it held true in both posterior cerebral (data not shown) and cremaster muscle resistance vessels (Figure 4). Our molecular studies of this model further defined (4) that its vascular phenotype may at least partly depend on enhanced activities of p38 MAPK and ERK1/2 and their ability to effect (5) inactivating phosphorylation of MYPT1, the regulatory subunit of MLCP. Although links between S1P and activation of both p38 MAPK and ERK1/2 have been established in smooth muscle,<sup>34,35</sup> our finding of complete susceptibility of the enhanced myogenic response in chronic HF to a p38 MAPK inhibitor is of particular therapeutic interest. Taken together, this study brings forth a fundamental mechanism underlying the chronically elevated PR observed in HF and provides new testable targets.

In this study, we used an established model of MI-induced HF in mice.<sup>36</sup> LAD ligation resulted in  $\approx 30\%$  infarct of the left ventricle, resulting in all the hallmarks of HF (Table), including calculated increases in PR consistent with previous reports.<sup>7</sup> Increased vascular tone and PR may stem from alterations in resistance artery structure and/or function. Indeed, indirect evidence of altered vascular structure has been reported in human subjects with HF.<sup>37,38</sup> However, in

the relatively short-term (12 weeks) model studied here, we failed to detect any significant structural changes in mesenteric arteries isolated from mice with HF. As such, we believe that vascular remodeling contributes minimally to the observed increases in vascular tone at these stages, and that the elevations in PR described are based primarily on functional perturbations.

To explore the latter, we performed extensive vasomotor analyses. Near identical PE and NEPI dose-response relationships for mesenteric and cremaster arteries respectively from mice with established HF and sham indicated that enhanced adrenergic sensitivity is not responsible for chronically elevated PR of HF. We also excluded reduced responsiveness of mesenteric arteries to endothelium-derived (ACh) or exogenous (SNP) sources of nitric oxide, a finding consistent with a report in rat, in which endothelium-derived mediators were found not to account for differences in myogenic responses in HF.<sup>7</sup> However, as “endothelial dysfunction” has been documented in conduit brachial arteries of patients with chronic HF,<sup>39</sup> the absence of impaired ACh-induced vasodilation in our model was unexpected, and may reflect pathophysiological differences between species, conduit versus resistance arteries, or the relatively short-term nature of our model. We have also not excluded the possibility of a HF-associated shift from NO to EDHF (endothelium-derived hyperpolarizing factor) as the dominant endothelium-derived vasodilator,<sup>40</sup> and further studies examining flow-mediated vasodilation are required to probe this issue further.

The regulation of myogenic response represents an additional distinct means of modulating vascular function. Myogenic mechanisms are capable of efficiently maintaining elevated levels of vascular tone over an extended period of time, because they: (1) do not require systemic neurohumoral activation; (2) can be controlled locally; and (3) can uncouple the  $\text{Ca}^{2+}$  signal from vasoconstriction over time.<sup>21</sup> Accordingly, the majority of PE-mediated increases in MAP in conscious dogs<sup>14</sup> (and hamsters<sup>41</sup>) has been shown to depend on a myogenic mechanism.<sup>13,14,42</sup>

As hypothesized, mesenteric arteries from mice with post-MI HF displayed a dramatic increase in myogenic response as compared to controls. This may explain the increased PR observed in mice with HF in vivo, in the absence of any overt alteration in the  $\text{Ca}^{2+}$  sensitivity of isolated mesenteric arteries. As a methodological note, the present experimental model maintained constant pressure when vasomotor responses were elicited (ie, there was no systemic pressure on which the myogenic tone would exert feedback). Thus, the observed enhancement in myogenic tone would not be observed in (or explain) any of the ligand dose-response experiments.

The regulation of myogenic tone involves both  $\text{Ca}^{2+}$ -dependent (transmembrane  $\text{Ca}^{2+}$  flux) and  $\text{Ca}^{2+}$ -independent (RhoA signaling) mechanisms.<sup>21</sup> Mediators that orchestrate these two fundamental processes thus represent master controls that ultimately determine the extent of the myogenic response. We have previously shown that S1P signaling plays a central role in regulating the myogenic response of hamster skeletal muscle arteries, where it modulates both pressure-stimulated elevations in intracellular  $\text{Ca}^{2+}$  and  $\text{Ca}^{2+}$ -

independent mechanisms. The latter are attributed to extracellular S1P, which is synthesized and released by *Sphk1* in response to pressure elevations and acts via the S1P<sub>2</sub>R to activate RhoA/Rho kinase<sup>17</sup> and Rac1<sup>20</sup> signaling cascades to ultimately inhibit MLCP. It is noteworthy, that of the three vascular S1P receptor subtypes (S1P<sub>1</sub>-, S1P<sub>2</sub>- and S1P<sub>3</sub>-),<sup>43,44</sup> mouse mesenteric arteries as well as isolated VSMCs from mouse mesenteric arteries (where contamination by endothelial mRNA can be excluded) predominantly express S1P<sub>2</sub>R mRNA (Online Figure VI, B).

However, in terms of regulating myogenic response of mouse mesenteric arteries, S1P/S1P<sub>2</sub>R signaling appears to be of limited significance in sham controls, where S1P<sub>2</sub>R blockade attenuated myogenic response by only  $\approx 30\%$ . This result was unexpected, as we had previously shown that S1P is a critical regulator of myogenic response in hamster.<sup>17</sup> In this prior study, hamster skeletal muscle arteries were transfected with a dominant-negative mutant of *Sphk1* (*Sphk1*<sup>G82D</sup>)<sup>45</sup> and a distinct “1-step” perfusion pressure protocol to induce myogenic response was used.<sup>17</sup> Thus, to obviate methodological differences, we tested myogenic response via the 1-step protocol in mesenteric arteries isolated from *Sphk1*<sup>-/-</sup> mice (see the Online Data Supplement). Our finding that myogenic responses were similar in *Sphk1*<sup>-/-</sup> and wild-type vessels suggests that genetic absence of *Sphk1* throughout development can be completely compensated for.

In stark contrast to vessels from sham controls, S1P/S1P<sub>2</sub>R signaling dominates the regulation of myogenic response in mesenteric arteries of mice with HF, as manifest by the complete abrogation of myogenic responses following S1P<sub>2</sub>R blockade with JTE013 in mice 2 or more weeks after LAD ligation (Figure 3B through 3D). Mesenteric artery vasoconstriction in response to exogenously applied S1P is also dramatically enhanced in HF (Figure 4), a result consistent with the emerging importance of S1P in the regulation of myogenic responses. It is worth noting that the shift toward a dominant role for S1P signaling in the regulation of myogenic responses is not immediate. Despite clearly increased myogenic responses (and PR, see Online Figure I) at 1 week after LAD ligation, the relative contribution of S1P/S1P<sub>2</sub>R signaling at this early stage is similar to that of controls (Figure 3A). Indeed, there is substantial evidence for sympathetic activation in the early stages of HF,<sup>46</sup> and our own observation of reduced responses to PE at lower (ie, physiological) doses at 1 week after MI may suggest “desensitization” over physiological concentrations even though the experimental EC<sub>50</sub> appeared unchanged (Figure 2A). Further attesting to the critical importance of S1P/S1P<sub>2</sub>R in inducing and or maintaining elevated PR in HF, we failed to document any differences in myogenic response between sham and HF mice lacking *Sphk1* (*Sphk1*<sup>-/-</sup>), *Sphk1* and one allele of *Sphk2* (*Sphk1*<sup>-/-</sup>/*Sphk2*<sup>+/-</sup>; the double knockout being embryonic lethal), and S1P<sub>2</sub>R (S1P<sub>2</sub>R<sup>-/-</sup>) (Online Figure VII). Indeed, future studies aimed at determining other systemic (ie, “nonmyogenic” or “nonmesenteric”) mechanisms by which *Sphk1*<sup>-/-</sup>/*Sphk2*<sup>+/-</sup> mice increase PR during HF may be of particular interest (Online Figure VIII).

Although S1P is capable of regulating Ca<sup>2+</sup>-dependent and -independent mechanisms, both of which govern the

myogenic response,<sup>21</sup> our data from this HF model suggest that Ca<sup>2+</sup>-independent mechanisms predominate. By definition, Ca<sup>2+</sup> sensitivity of the contractile apparatus reflects the ratio of activities of MLCK to MLCP.<sup>26</sup> The balance between MLCK and MLCP ultimately dictates the phosphorylation status of MLC<sub>20</sub>, which controls contraction. MLCK activity is dependent on intracellular Ca<sup>2+</sup> levels ([Ca<sup>2+</sup>]<sub>i</sub>),<sup>26</sup> whereas the modulation of MLCP activity allows the phosphorylation status of MLC<sub>20</sub> to be altered independent of [Ca<sup>2+</sup>]<sub>i</sub>. The inherent advantage of uncoupling contraction from [Ca<sup>2+</sup>]<sub>i</sub> is that chronic vascular tone can be maintained at resting Ca<sup>2+</sup> levels; conserving energy-requiring Ca<sup>2+</sup> cycling for other critical processes.

Several lines of experimental evidence support the notion that Ca<sup>2+</sup>-independent mechanisms are key to maintaining PR in mesenteric arteries from mice with HF: (1) greater abundance of Ser19-phosphorylated MLC<sub>20</sub>; (2) greater abundance of Thr850-phosphorylated MYPT1, the inactivating subunit of MLCP; (3) dramatically decreased Rho-kinase activity, which is normally a key mediator of enhanced Ca<sup>2+</sup> sensitivity; and (4) an unaltered [Ca<sup>2+</sup>]<sub>ext</sub>-vessel diameter relationship, together implicating a heretofore unrecognized “Rho-independent” mechanism for the inhibition of MLCP activity in resistance arteries in HF. Finally (5), the findings of increased p38 MAPK and ERK1/2 activation in mesenteric arteries of HF animals, and (6) the ability of a p38 MAPK inhibitor to abolish the increased myogenic response of HF but not sham arteries (Figure 7) shed new light on the pathways involved in maintaining elevated PR. Although the p38 MAPK inhibitor had little (if any) effect on the myogenic response of mesenteric arteries from sham animals, the same inhibitor has been shown to blunt myogenic responses of rat skeletal muscle arterioles.<sup>47</sup> Together, these data suggest that p38 MAPK exerts species/vessel- and disease-specific influence on the myogenic response.

Finally, “upstream” signals that may have led to the adaptive shifts in vasomotor function observed in our model of HF are worthy of discussion. For example, Gschwend et al showed that blockade of AT<sub>1</sub> receptors with angiotensin receptor blockers reversed the increased myogenic constriction observed in HF in rat,<sup>7</sup> suggesting participation of RAS, which has also been linked directly (and indirectly via NADPH oxidase-derived ROS<sup>48</sup>) to *Sphk*-dependent vasomotor effects in isolated vessel preparations from nondiseased animals<sup>20,49</sup> and to p38 MAPK activation in VSMCs.<sup>48</sup> Further studies will be needed to dissect the precise contributions of RAS, other neurohormones, or even cytokines implicated in HF such as tumor necrosis factor- $\alpha$ ,<sup>50</sup> to *Sphk* activity,<sup>51,52</sup> S1P receptor expression,<sup>52</sup> and myogenic responses.

In summary, we have shown that the myogenic response is strongly augmented in mesenteric, posterior cerebral, and cremaster muscle arteries from mice with HF. As HF progresses, S1P/S1P<sub>2</sub>R signaling emerges as a dominant mechanism regulating this increased myogenic response, acting via inhibited MLCP activity and possibly via enhanced activation of p38 MAPK and ERK1/2, known activators of the inhibitory effects of ZIPK and ILK on the MYPT1 subunit of MLCP in smooth muscle. Because this is a

potentially critical mechanism that serves to increase vascular tone on a chronic basis, it may represent a novel therapeutic target for the treatment of HF. Indeed, the functional effects of a p38 MAPK inhibitor on myogenic responses in HF, as but one example of a drug target in the pathway identified, strongly supports this notion.

### Acknowledgments

We thank Yohr Takuwa (Kanazawa University, Japan) for the gift of pGEX-2T/GST-RBD and Richard Proia (NIH, Bethesda, Md) for providing *Sphk1*<sup>-/-</sup>, *Sphk1*<sup>-/-</sup>/*Sphk2*<sup>+/-</sup>, and *S1P<sub>2</sub>R*<sup>-/-</sup> mice.

### Sources of Funding

M.A.A. was supported by training awards from the Cell Biology of Atherosclerosis program of the Heart and Stroke Foundation of Ontario (HSFO) (5738) and from the TACTICS program of the Canadian Institutes of Health Research (CIHR) (53900) and by the Heart and Stroke Richard Lewar Centre of Excellence. S.-S.B. holds a New Investigator Award of the HSFO. M.H. is a Career Investigator of the HSFO (CI 5503). This work was supported by CIHR operating grants FRN 117801 (to M.H.) and MOP-84402 (to S.-S.B.) and a Canadian Foundation for Innovation/Ontario Research Fund award (11810) (to S.-S.B.).

### Disclosures

None.

### References

- He J, Ogen LG, Bazzano LA, Vupputuri S, Loria C, Whelton PK. Risk factors for congestive heart failure in US men and women: NHANES I epidemiologic follow-up study. *Arch Intern Med*. 2001;161:996–1002.
- Zelis R, Flaim SF. Alterations in vasomotor tone in congestive heart failure. *Prog Cardiovasc Dis*. 1982;24:437–459.
- Zelis R, Flaim SF. The circulations in congestive heart failure. *Mod Concepts Cardiovasc Dis*. 1982;51:79–84.
- Schrier RW, Abraham WT. Hormones and hemodynamics in heart failure. *N Engl J Med*. 1999;341:577–585.
- Frohlich ED, Tarazi RC, Ulrych M, Dustan HP, Page IH. Tilt test for investigating a neural component in hypertension. Its correlation with clinical characteristics. *Circulation*. 1967;36:387–393.
- Leimbach WN Jr, Wallin BG, Victor RG, Aylward PE, Sundlof G, Mark AL. Direct evidence from intraneural recordings for increased central sympathetic outflow in patients with heart failure. *Circulation*. 1986;73:913–919.
- Gschwend S, Henning RH, Pinto YM, de ZD, van Gilst WH, Buikema H. Myogenic constriction is increased in mesenteric resistance arteries from rats with chronic heart failure: instantaneous counteraction by acute AT1 receptor blockade. *Br J Pharmacol*. 2003;139:1317–1325.
- Liggett SB, Mialet-Perez J, Thaneemit-Chen S, Weber SA, Greene SM, Hodne D, Nelson B, Morrison J, Domanski MJ, Wagoner LE, Abraham WT, Anderson JL, Carlucci JF, Krause-Steinrauf HJ, Lazzeroni LC, Port JD, Lavori PW, Bristow MR. A polymorphism within a conserved beta(1)-adrenergic receptor motif alters cardiac function and beta-blocker response in human heart failure. *Proc Natl Acad Sci U S A*. 2006;103:11288–11293.
- Meredith IT, Broughton A, Jennings GL, Esler MD. Evidence of a selective increase in cardiac sympathetic activity in patients with sustained ventricular arrhythmias. *N Engl J Med*. 1991;325:618–624.
- Takahashi M, Yamada T, Kinoshita M. [Catecholamines and beta-blockers for the treatment of heart failure]. *Nippon Rinsho*. 1993;51:1268–1275.
- Feng QP, Bergdahl A, Lu XR, Sun XY, Edvinsson L, Hedner T. Vascular alpha-2 adrenoceptor function is decreased in rats with congestive heart failure. *Cardiovasc Res*. 1996;31:577–584.
- Kiuchi K, Sato N, Shannon RP, Vatner DE, Morgan K, Vatner SF. Depressed beta-adrenergic receptor- and endothelium-mediated vasodilation in conscious dogs with heart failure. *Circ Res*. 1993;73:1013–1023.
- Metting PJ, Kostrzewski KA, Stein PM, Stoos BA, Britton SL. Quantitative contribution of systemic vascular autoregulation in acute hypertension in conscious dogs. *J Clin Invest*. 1989;84:1900–1905.
- Metting PJ, Stein PM, Stoos BA, Kostrzewski KA, Britton SL. Systemic vascular autoregulation amplifies pressor responses to vasoconstrictor agents. *Am J Physiol*. 1989;256:R98–R105.
- Bolz SS, Pieperhoff S, de WC, Pohl U. Intact endothelial and smooth muscle function in small resistance arteries after 48 h in vessel culture. *Am J Physiol Heart Circ Physiol*. 2000;279:H1434–H1439.
- Bolz SS, Pohl U. Highly effective non-viral gene transfer into vascular smooth muscle cells of cultured resistance arteries demonstrated by genetic inhibition of sphingosine-1-phosphate-induced vasoconstriction. *J Vasc Res*. 2003;40:399–405.
- Bolz SS, Vogel L, Sollinger D, Derwand R, Boer C, Pitson SM, Spiegel S, Pohl U. Sphingosine kinase modulates microvascular tone and myogenic responses through activation of RhoA/Rho kinase. *Circulation*. 2003;108:342–347.
- Gros R, Van WR, You X, Thorin E, Husain M. Effects of age, gender, and blood pressure on myogenic responses of mesenteric arteries from C57BL/6 mice. *Am J Physiol Heart Circ Physiol*. 2002;282:H380–H388.
- Gros R, Afroze T, You XM, Kabir G, Van WR, Kalair W, Hoque AE, Mungrue IN, Husain M. Plasma membrane calcium ATPase overexpression in arterial smooth muscle increases vasomotor responsiveness and blood pressure. *Circ Res*. 2003;93:614–621.
- Keller M, Lidington D, Vogel L, Peter BF, Sohn HY, Pagano PJ, Pitson S, Spiegel S, Pohl U, Bolz SS. Sphingosine kinase functionally links elevated transmural pressure and increased reactive oxygen species formation in resistance arteries. *FASEB J*. 2006;20:702–704.
- Schubert R, Lidington D, Bolz SS. The emerging role of Ca<sup>2+</sup> sensitivity regulation in promoting myogenic vasoconstriction. *Cardiovasc Res*. 2008;77:8–18.
- Sakurada S, Okamoto H, Takuwa N, Sugimoto N, Takuwa Y. Rho activation in excitatory agonist-stimulated vascular smooth muscle. *Am J Physiol Cell Physiol*. 2001;281:C571–C578.
- Noyan-Ashraf MH, Momen MA, Ban K, Sadi AM, Zhou YQ, Riazi AM, Baggio LL, Henkelman RM, Husain M, Drucker DJ. GLP-1R agonist liraglutide activates cytoprotective pathways and improves outcomes after experimental myocardial infarction in mice. *Diabetes*. 2009;58:975–983.
- Mungrue IN, Gros R, You X, Pirani A, Azad A, Csont T, Schulz R, Butany J, Stewart DJ, Husain M. Cardiomyocyte overexpression of iNOS in mice results in peroxynitrite generation, heart block, and sudden death. *J Clin Invest*. 2002;109:735–743.
- Jackson PA, Duling BR. Myogenic response and wall mechanics of arterioles. *Am J Physiol*. 1989;257:H1147–H1155.
- Somlyo AP, Somlyo AV. Ca<sup>2+</sup> sensitivity of smooth muscle and non-muscle myosin II: modulated by G proteins, kinases, and myosin phosphatase. *Physiol Rev*. 2003;83:1325–1358.
- Sakurada S, Takuwa N, Sugimoto N, Wang Y, Seto M, Sasaki Y, Takuwa Y. Ca<sup>2+</sup>-dependent activation of Rho and Rho kinase in membrane depolarization-induced and receptor stimulation-induced vascular smooth muscle contraction. *Circ Res*. 2003;93:548–556.
- Kitazawa T, Eto M, Woodsome TP, Brautigan DL. Agonists trigger G protein-mediated activation of the CPI-17 inhibitor phosphoprotein of myosin light chain phosphatase to enhance vascular smooth muscle contractility. *J Biol Chem*. 2000;275:9897–9900.
- Niirio N, Ikebe M. Zipper-interacting protein kinase induces Ca(2+)-free smooth muscle contraction via myosin light chain phosphorylation. *J Biol Chem*. 2001;276:29567–29574.
- Deng JT, Van Lierop JE, Sutherland C, Walsh MP. Ca<sup>2+</sup>-independent smooth muscle contraction: a novel function for integrin-linked kinase. *J Biol Chem*. 2001;276:16365–16373.
- Cao W, Sohn UD, Bitar KN, Behar J, Biancani P, Harnett KM. MAPK mediates PKC-dependent contraction of cat esophageal and lower esophageal sphincter circular smooth muscle. *Am J Physiol Gastrointest Liver Physiol*. 2003;285:G86–G95.
- Harnett KM, Cao W, Biancani P. Signal-transduction pathways that regulate smooth muscle function I. Signal transduction in phasic (esophageal) and tonic (gastroesophageal sphincter) smooth muscles. *Am J Physiol Gastrointest Liver Physiol*. 2005;288:G407–G416.
- Ihara E, Moffat L, Ostrander J, Walsh MP, MacDonald JA. Characterization of protein kinase pathways responsible for Ca<sup>2+</sup> sensitization in rat ileal longitudinal smooth muscle. *Am J Physiol Gastrointest Liver Physiol*. 2007;293:G699–G710.
- Usui S, Sugimoto N, Takuwa N, Sakagami S, Takata S, Kaneko S, Takuwa Y. Blood lipid mediator sphingosine 1-phosphate potently stimulates platelet-derived growth factor-A and -B chain expression through

- S1P1-Gi-Ras-MAPK-dependent induction of Kruppel-like factor 5. *J Biol Chem*. 2004;279:12300–12311.
35. Rakhit S, Conway AM, Tate R, Bower T, Pyne NJ, Pyne S. Sphingosine 1-phosphate stimulation of the p42/p44 mitogen-activated protein kinase pathway in airway smooth muscle. Role of endothelial differentiation gene 1, c-Src tyrosine kinase and phosphoinositide 3-kinase. *Biochem J*. 1999;338:643–649.
  36. Salto-Tellez M, Yung Lim S, El-Oakley RM, Tang TP, ALmsherqi ZA, Lim SK. Myocardial infarction in the C57BL/6J mouse: a quantifiable and highly reproducible experimental model. *Cardiovasc Pathol*. 2004; 13:91–97.
  37. Houben AJ, Beljaars JH, Hofstra L, Kroon AA, de Leeuw PW. Microvascular abnormalities in chronic heart failure: a cross-sectional analysis. *Microcirculation*. 2003;10:471–478.
  38. Mengden T, Douven C, Vetter H, Dusing R. Evidence for structural alterations in resistance arteries of patients with severe congestive heart failure. *J Vasc Res*. 1999;36:229–234.
  39. Ferrari R, Bachetti T, Agnoletti L, Comini L, Curello S. Endothelial function and dysfunction in heart failure. *Eur Heart J*. 1998;19:G41–G47.
  40. Katz SD, Krum H. Acetylcholine-mediated vasodilation in the forearm circulation of patients with heart failure: indirect evidence for the role of endothelium-derived hyperpolarizing factor. *Am J Cardiol*. 2001;87: 1089–1092.
  41. de WC, Jahrbeck B, Schafer C, Bolz SS, Pohl U. Nitric oxide opposes myogenic pressure responses predominantly in large arterioles in vivo. *Hypertension*. 1998;31:787–794.
  42. de WC, Bolz SS, Kaas J, Pohl U. Myogenic effects enhance norepinephrine constriction: inhibition by nitric oxide and felodipine. *Kidney Int Suppl*. 1998;67:S122–S126.
  43. Hla T, Lee MJ, Ancellin N, Paik JH, Kluk MJ. Lysophospholipids–receptor revelations. *Science*. 2001;294:1875–1878.
  44. Rosen H, Goetzl EJ. Sphingosine 1-phosphate and its receptors: an autocrine and paracrine network. *Nat Rev Immunol*. 2005;5:560–570.
  45. Pitson SM, Moretti PA, Zebol JR, Xia P, Gamble JR, Vadas MA, D'Andrea RJ, Wattenberg BW. Expression of a catalytically inactive sphingosine kinase mutant blocks agonist-induced sphingosine kinase activation. A dominant-negative sphingosine kinase. *J Biol Chem*. 2000; 275:33945–33950.
  46. Esler M, Kaye D, Lambert G, Esler D, Jennings G. Adrenergic nervous system in heart failure. *Am J Cardiol*. 1997;80:7L–14L.
  47. Massett MP, Ungvari Z, Csiszar A, Kaley G, Koller A. Different roles of PKC and MAP kinases in arteriolar constrictions to pressure and agonists. *Am J Physiol Heart Circ Physiol*. 2002;283:H2282–H2287.
  48. Touyz RM. Reactive oxygen species, vascular oxidative stress, and redox signaling in hypertension: what is the clinical significance? *Hypertension*. 2004;44:248–252.
  49. Mulders AC, Hendriks-Balk MC, Mathy MJ, Michel MC, Alewijnse AE, Peters SL. Sphingosine kinase-dependent activation of endothelial nitric oxide synthase by angiotensin II. *Arterioscler Thromb Vasc Biol*. 2006; 26:2043–2048.
  50. Sekiguchi K, Li X, Coker M, Flesch M, Barger PM, Sivasubramanian N, Mann DL. Cross-regulation between the renin-angiotensin system and inflammatory mediators in cardiac hypertrophy and failure. *Cardiovasc Res*. 2004;63:433–442.
  51. Mastrandrea LD, Sessanna SM, Laychock SG. Sphingosine kinase activity and sphingosine-1 phosphate production in rat pancreatic islets and INS-1 cells: response to cytokines. *Diabetes*. 2005;54:1429–1436.
  52. Chen XL, Grey JY, Thomas S, Qiu FH, Medford RM, Wasserman MA, Kunsch C. Sphingosine kinase-1 mediates TNF-alpha-induced MCP-1 gene expression in endothelial cells: upregulation by oscillatory flow. *Am J Physiol Heart Circ Physiol*. 2004;287:H1452–H1458.

## Novelty and Significance

### What Is Known?

- In heart failure, an increase in peripheral resistance maintains an acceptable blood pressure despite diminished cardiac output but increases the afterload against which the compromised heart must work.
- The myogenic response, a primary intrinsic mechanism that regulates resistance artery tone, is augmented in heart failure.

### What New Information Does This Article Contribute?

- Increased myogenic responsiveness in heart failure results from an upregulation of microvascular sphingosine-1-phosphate (S1P) signaling, which, in turn, activates the extracellular signal-regulated kinase (ERK)1/2 and p38 mitogen-activated protein kinase (MAPK) pathways that ultimately inhibit myosin light chain phosphatase.
- Microvascular S1P signaling is a potential therapeutic target for the control of peripheral resistance in heart failure.

This study demonstrates that microvascular S1P signaling is the primary molecular pathway that underlies increased myogenic responsiveness in heart failure. In mesenteric, cerebral, and cremaster vascular beds, S1P becomes the primary long-term modulator of myogenic responsiveness within 2 weeks of heart failure onset. This switch toward S1P signaling likely replaces an initial sympathetic stimulus. Animals lacking components of the S1P signaling pathway do not show increased myogenic tone in heart failure. ERK1/2 and p38 MAPK are downstream targets of S1P that collectively contribute to the inhibition of MLCP, which promotes myogenic vasoconstriction. These results reveal a dynamic microvascular adaptation to heart failure. Investigation into the mechanisms that promote this adaptive response is warranted. Our most significant finding is the identification of S1P signaling as a potential therapeutic target for the control of peripheral resistance in heart failure.

## SUPPLEMENT MATERIAL

### SUPPLEMENTARY MATERIALS & METHODS

**Reagents:** Other reagents included complete protease (Roche) and phosphatase (Cedarlane) inhibitor cocktail tablets. Abs to MLC-20, phospho-MLC-20 (Ser19), p38 MAPK and phospho-p38 MAPK (Thr180/Tyr182), ERK1/2 (p44/42 MAPK), phospho-ERK1/2 (Thr202/Tyr204) and ILK were from Cell Signaling. Rabbit polyclonal Abs to phospho-MYPT1 (Thr850), MYPT1, and phospho-CPI-17 (Thr38) were from Upstate, and to zipper interacting protein kinase (ZIPK) was from ProSci Inc. Mouse mAbs to RhoA and CPI-17 were from Santa Cruz. HRP-conjugated secondary Abs against rabbit (Santa Cruz) and mouse (Pierce) Abs were used.

**Echocardiography:** LV-end-diastolic (LVEDD) and -end-systolic dimensions (LVESD) were obtained. Fractional shortening (FS) was defined as  $[(LVEDD-LVESD)/LVEDD] \times 100$ . LV ejection fraction (LVEF) was defined as  $[(LVEDD^3-LVESD^3)/LVEDD^3] \times 100$ . Aortic flow velocity-time integral (VTI) was measured using pulse wave Doppler just above the aortic root. Aortic cross-sectional area (CSA) was calculated from the aortic root dimension (AoD):  $CSA = (AoD/2)^2 \times \pi$ . Stroke volume (SV), cardiac output (CO), and peripheral resistance (PR) were calculated as:  $SV = CSA \times \text{Aortic VTI}$ ;  $CO = SV \times HR$ ;  $PR = MAP/CO$ . For all measurements, three beats were averaged for each parameter.

**Histological analysis:** Following euthanasia, hearts were removed, fixed in 10% formaldehyde and paraffin embedded. Slices (10  $\mu\text{m}$ ) were stained with H&E. The circumferential length of the infarct was measured and compared to total myocardial length; the resulting percentage was used as an index of infarct size. Second-order mesenteric arteries were isolated, cleared of fat and fixed in formalin overnight before being embedded in paraffin, sectioned into 4  $\mu\text{m}$  slices and stained with H&E, Picrosirius red and Masson's trichrome. Images of stained sections were obtained with a Leica DMLB microscope equipped with a Photometrics Cool-Snap digital camera (Carsen Group). Mean luminal and medial areas were assessed by averaging triplicate values at the proximal, middle, and distal thirds of the collected samples.

**VSMC isolation and culture:** Following removal of adjacent connective and fatty tissue, MA segments were cut into small pieces and incubated for 30 min at 37°C in 0.25% Trypsin gently bubbled with 100% O<sub>2</sub>. After incubation, the supernatant was removed and the tissues were placed in 1 ml HEPES buffer #1 [mM: NaCl 126, KCl 6, HEPES 10, Taurine 20, Glucose 20, Pyruvate 5, MgCl<sub>2</sub> 1, containing mg: collagenase IV-S 2, papain 1, and Dithiothreitol (DTT) 1.5, with 70  $\mu\text{l}$  elastase] for 40 min. Supernatant was removed and the tissues were triturated using a small pipette in HEPES buffer #2 [mM: NaCl 141, KCl 4.7, CaCl<sub>2</sub> 1.8, MgCl<sub>2</sub> 1.2, HEPES 10, Glucose 10]. The cell solution was washed 3X with PBS under sterile conditions and transferred to culture media of DMEM containing 10% heat-inactivated FCS and 1% Penicillin-Streptomycin in a humidified incubator supplied with 5% CO<sub>2</sub> at 37°C.

**Molecular analysis of contractile proteins and regulatory signaling:** Protein extracts of MA underwent Western blot to measure MLCK-dependent activation (i.e. Ser-19 phosphorylation) of the principal regulatory contractile protein MLC. MA from animals 6 wks post-op were fixed in a slurry of acetone dry ice and solubilized in urea sample buffer<sup>1</sup>. Extracts were mixed with 4X Laemmli's SDS buffer and run on a 4-12% gradient gel. Following transfer to PVDF, membranes were probed with Abs to MLC-20 (Cat # 3672) and phospho-MLC-20 (Cat # 3671). Western blots for inactive (phosphorylated) and total MYPT1, and active (phosphorylated) and total CPI-17 were also performed. MA were fixed in a slurry of acetone dry ice containing 20 mM DTT and 10% TCA and washed in acetone containing 10 mM DTT at room temperature. Fixed tissues were homogenized in a buffer [mM: Tris/HCl 20, pH 7.5; NaF 100; Na<sub>3</sub>VO<sub>4</sub> 1; SDS 0.1%; EGTA 2; NP-40 0.5%; 1X protease and phosphatase inhibitor cocktails each; and PMSF 1]. For the Rho assay, MA were fixed in liquid N<sub>2</sub> and homogenized in lysis buffer [mM: Tris HCL, pH 7.2 50, NaCl 500, MgCl<sub>2</sub> 10, Triton X-100 1%, deoxycholic acid 0.5%, SDS 0.1%, complete protease inhibitor 1X, phosphatase inhibitor cocktail 1X, PMSF 1]. Homogenates were centrifuged at 15,000 rpm at 4°C for 10 min, and a portion of the supernatant was assayed by the bicinchoninate assay. For the Rho assay, supernatants (180 $\mu\text{g}$ ) were then incubated with glutathione S-transferase-Rhotekin immobilized on 4B beads (GE Healthcare,

Little Chalfont, Buckinghamshire, UK) at 4°C for 30 min. Beads were washed twice with a buffer [mM: Tris/HCl 50, pH 7.2, Triton X-100 1%, NaCl 150, and MgCl<sub>2</sub> 10]. Bead-bound RhoA was solubilized with Laemmli's SDS sample buffer, heated at 70°C for 5 min, run on a 4-12% acrylamide gradient gel, transferred to a PVDF membrane, and probed with anti-Rho Ab (Cat# sc-418). For Western blot of ZIPK, ILK, p38 MAPK and ERK1/2, supernatants (15-25 µg) were run on 4-12% gradient gels, transferred to PVDF and probed with anti-ZIPK (Cat# 2067), anti-ILK (Cat# I-0783), anti-p38 MAPK (Cat# 9212), anti-phosphorylated p38 MAPK (Cat# 9211), anti-ERK1/2 (Cat# 4695), and anti-phospho-ERK1/2 (Cat# 9101). The amounts of phosphorylated-MLC, -MYPT1, -CPI-17, -p38 MAPK and -ERK1/2 were determined by densitometry, normalized to amounts of total MLC, MYPT1, CPI-17, p38 MAPK and ERK1/2 in each sample respectively, and expressed relative to the corresponding ratio found in MA from sham. Amounts of ZIPK, ILK and GTP-bound RhoA (GTP-Rho) were normalized for the amounts of α-SM-actin in each sample, and expressed relative to the ZIPK, ILK and GTP-Rho levels respectively in MA from sham-operated controls.

**PCR:** RNA from MA or primary VSMC was isolated using RNAeasy Kit (Qiagen). cDNA synthesis was performed using standard procedures. PCR was performed with primers for S1P<sub>1</sub>R forward 5'-GAA-CCA-TAA-CTC-TGT-GCC-TTT-GTC-TC-3', reverse 5'-TGA-GAG-ATC-ACA-ACA-CTT-CCT-CTT-G-3' (55°C, 395bp product); S1P<sub>2</sub>R forward 5'-GCA-GTG-ACA-AAA-GCT-GCC-GAA-TGC-TGA-TG-3', reverse 5'-AGA-TGG-TGA-CCA-CGC-AGA-GCA-CGT-AGT-G-3' (55°C, 170bp product); S1P<sub>3</sub>R forward 5'-TCA-GTA-TCT-TCA-CCG-CCA-TT-3', reverse 5'-AAT-CAC-TAC-GGT-CCG-CAG-AA-3' (55°C, 137bp product); GAPDH forward 5'-TTC-ACC-ACC-ATG-GAG-AAG-G-3', reverse 5'-CTC-GTG-GTT-CAC-ACC-CAT-C-3' (55°C, 111bp product) The PCR products were separated on a 2.5% agarose gel and analyzed with Image J software.

**Perfusion myography of mesenteric arteries:** Mice were euthanized by cervical dislocation. The mesentery was grossly dissected and placed in a Petri dish with ice-cold MOPS-buffered saline solution (MOPS buffer): [mM: NaCl 145, KCl 4.7, CaCl<sub>2</sub> 3, MgSO<sub>4</sub>•7H<sub>2</sub>O 1.17, NaH<sub>2</sub>PO<sub>4</sub>•2H<sub>2</sub>O 1.2, pyruvate 2, EDTA 0.02, MOPS 3, and Glucose 5.0]. Mesenteric arteries (MA; 2nd order, 150-200 µm) were dissected using a stereoscope and stored in ice-cold MOPS buffer for <6 h before experimentation. Vessels were mounted on a pressure myograph (Living Systems Instrumentation) which controls transmural pressure, maintains a constant temperature of 37°C and measures the luminal diameter of the vessel. Vessels were maintained at a transmural pressure of 60 mmHg for 30 min, changing MOPS buffer every 10 min. In all cases, transmural pressure was maintained at 60 mmHg. To assess the myogenic response, transmural pressure was increased in 20 mmHg steps from 20 to 120 mmHg. Vessel diameter (active) was measured at each pressure step once a steady state was reached (5-10 min). In some experiments, vessels were treated with JTE-013 (1 µM; 30 min) or SB203580 (5 µM; 30 min) following the myogenic response assessment and re-tested. At completion, passive diameter (dia<sub>passive</sub>) was recorded for each pressure step. Myogenic tone at each step was calculated as: (dia<sub>passive</sub>-dia<sub>active</sub>)/dia<sub>passive</sub>.

**One-step perfusion myography of *Sphk1*<sup>-/-</sup> mice:** MR in MA from *Sphk1* knockout mice was additionally assessed using a one-step protocol (i.e. transmural pressure was increased from 45 to 100 mmHg to elicit MR) and quantified as follows. The magnitude of MR was calculated as the percentage of constriction compared to the initial distension: (%)=(dia<sub>dist</sub>-dia<sub>t=7</sub>)/(dia<sub>dist</sub>-dia<sub>t=0</sub>)x100, where dia<sub>t=0</sub> is the diameter immediately preceding the pressure step, dia<sub>dist</sub> is the distended diameter immediately following the step, and dia<sub>t=7</sub> is the diameter measured 7 min following the step, an arbitrary time point where myogenic constriction is normally stable.

**Perfusion myography of cremaster muscle arteries:** Mice were anaesthetized with isoflurane and right and left cremaster arteries were exteriorized, excised and placed in 4°C MOPS buffer. Segments of the main arteriole were dissected as described<sup>2,3</sup>. Single arteries were cannulated with glass micropipettes and secured with silk suture (11-0) in a custom designed chamber. Chambers were transferred to the stage of an inverted microscope and arteries were pressurized to 60mmHg TMP and gradually warmed to 37°C. Vessels were set to *in vivo* length such that an increase in pressure to 100 mmHg did not cause lateral bowing of the segment. Perfusion baths were exchanged with MOPS and arteries were allowed to equilibrate over 30 min,

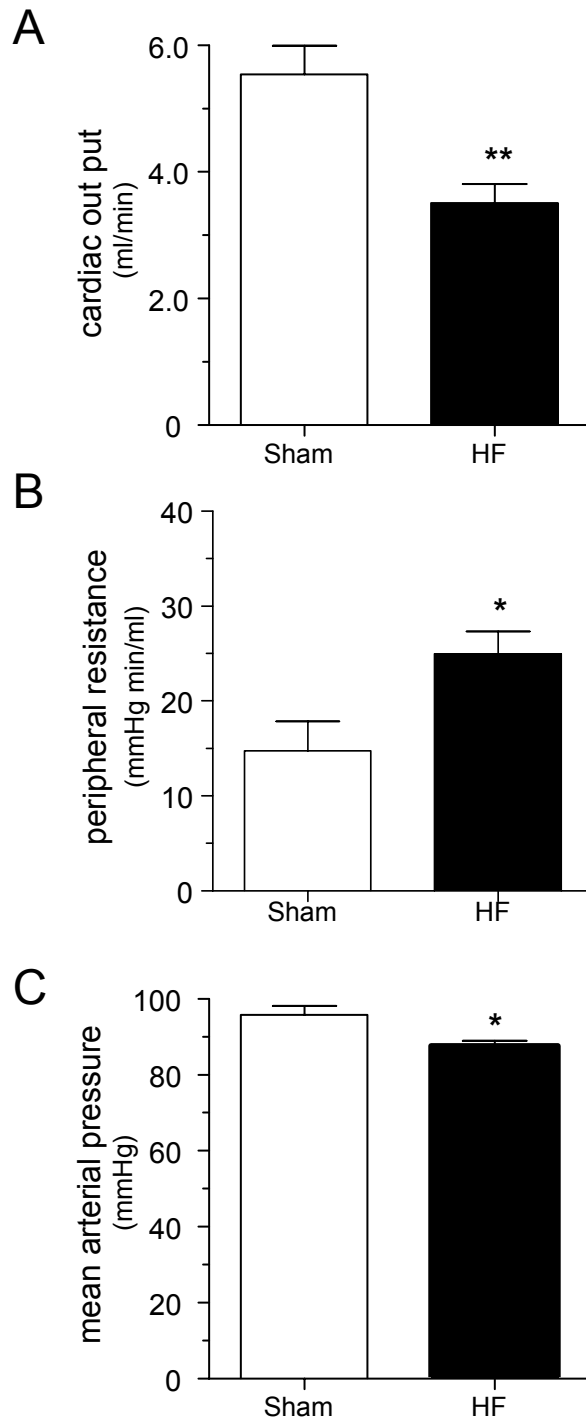
establishing spontaneous basal tone. All experiments were conducted at a TMP of 60 mmHg, with the exception of pressure-induced responses, which required a rapid change in pressure from 20-100 mmHg in 20 mmHg increments. Following equilibration, arteries were exposed to 0.3  $\mu$ M norepinephrine (NEPI) to test for viability. Arteries that did not constrict were excluded from analysis. Responses to changes in TMP (20-100 mmHg) and dose-responses to NEPI ( $10^{-10}$  to  $10^{-6}$  M) and S1P ( $10^{-9}$  to  $10^{-6}$  M) were compared to vessel diameter under 0 mM  $\text{Ca}^{2+}$  conditions. Outer diameter was measured using the Crescent Electronics video edge detector and was collected using PTI FeliX32 analysis Software (v1.2).

**Perfusion myography of posterior cerebral arteries:** Mice were anaesthetized with isoflurane and decapitated. The brain was rapidly removed from the cranium and immersed in ice-cold sterile MOPS buffer. Posterior cerebral artery segments (0.8-1.0mm in length) were carefully dissected from the surrounding connective tissue. Only 1<sup>st</sup> order vessels were isolated from mice (160-220 $\mu$ m). The isolated vessel segments were cannulated onto glass micropipettes, stretched to their *in vivo* lengths and pressurized as described above.

#### **SUPPLEMENTARY REFERENCES:**

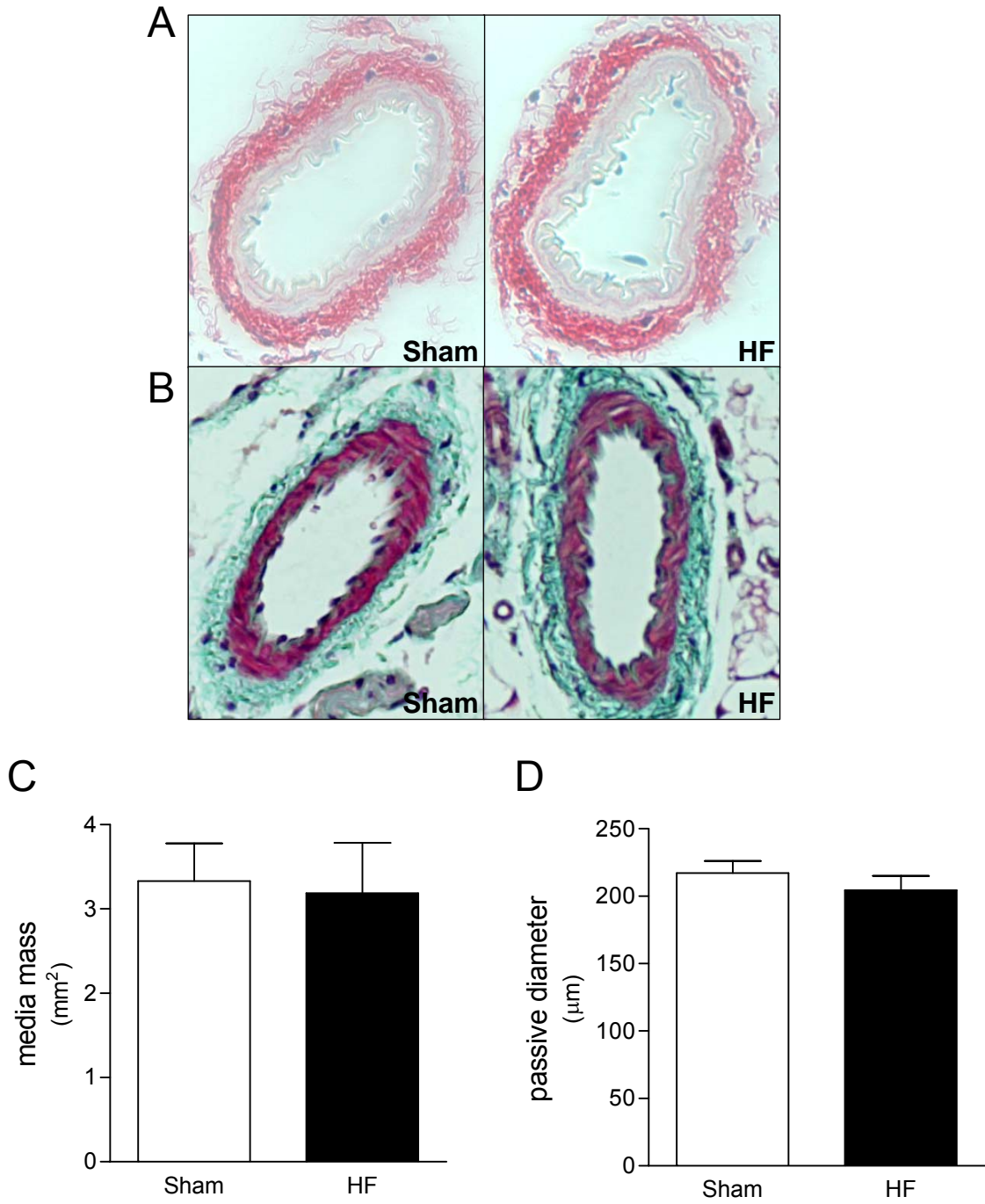
1. Kitazawa T, Eto M, Woodsome TP, Brautigan DL. Agonists trigger G protein-mediated activation of the CPI-17 inhibitor phosphoprotein of myosin light chain phosphatase to enhance vascular smooth muscle contractility. *J Biol Chem.* 2000;275:9897-9900.
2. Falcone JC, Davis MJ, Meininger GA. Endothelial independence of myogenic response in isolated skeletal muscle arterioles. *Am J Physiol.* 1991;260:H130-135.
3. Hill MA, Zou H, Davis MJ, Potocnik SJ, Price S. Transient increases in diameter and  $[\text{Ca}^{2+}]_i$  are not obligatory for myogenic constriction. *Am J Physiol Heart Circ Physiol.* 2000;278:H345-352.

# Online Figure I.



**Online Figure I: Hemodynamic parameters in HF mice.** Measurements of **(A)** cardiac output (CO), **(B)** peripheral resistance (PR) and **(C)** mean arterial pressure (MAP) in sham (n=5) and HF (n=6) mice at 1 wk post-op. MAP and CO were both reduced in HF vs. sham. PR was increased in HF vs. sham. Data are mean ± SE; \* $P < 0.05$ ; \*\* $P < 0.01$ .

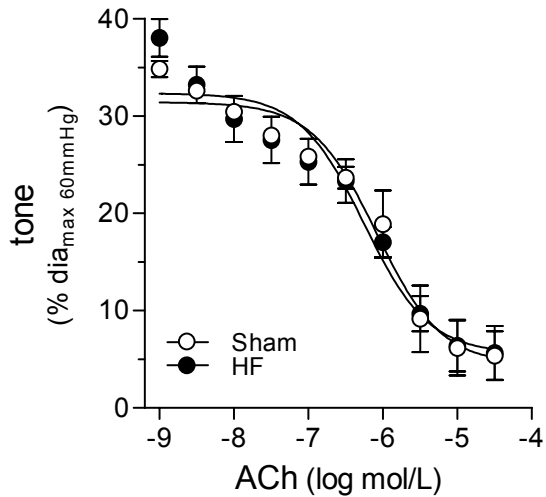
# Online Figure II.



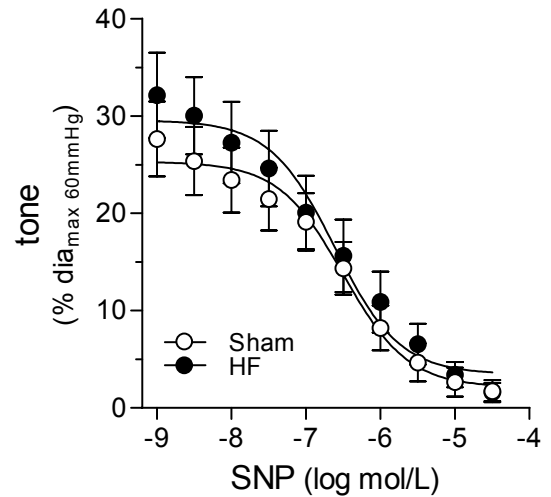
**Online Figure II: Histological analysis of resistance arteries from HF mice.** Representative micrographs of 2nd order mesenteric artery (MA) histological sections stained with **(A)** Picrosirius red and **(B)** Masson's trichrome are shown. Arteries from sham (left) and HF (right) animals did not display morphological differences. **(C)** Media mass and **(D)** maximal passive diameter did not differ in MA isolated from HF vs. sham mice. For each group, n≥5; data are mean ± SE; P=NS for all comparisons.

# Online Figure III.

A

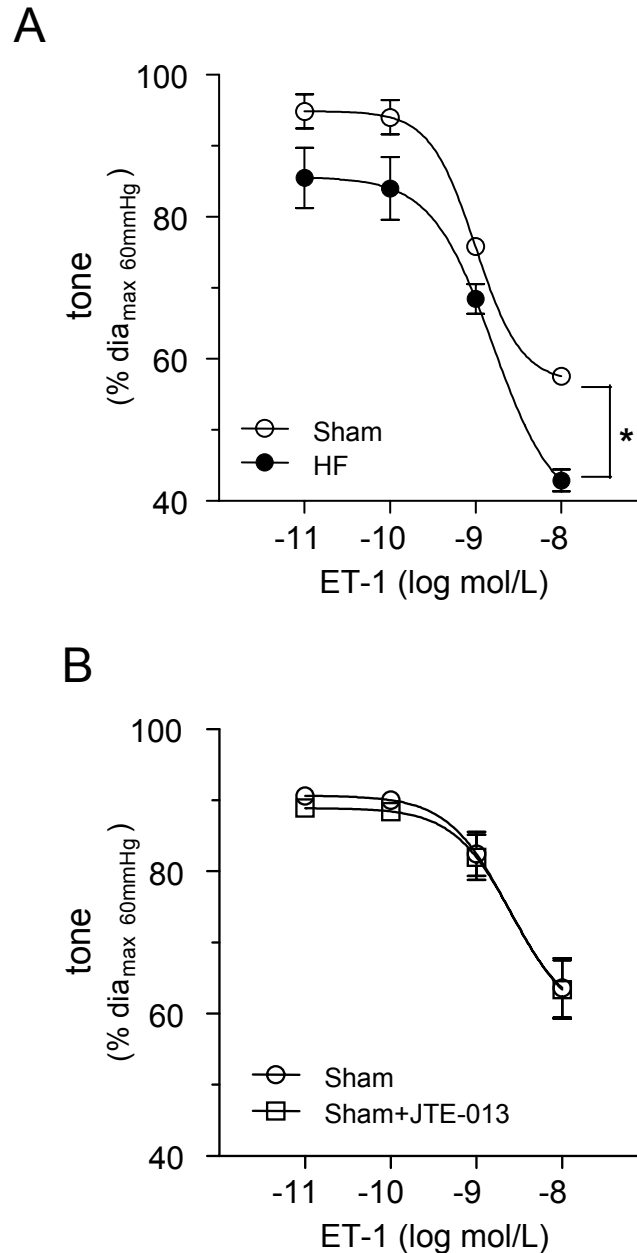


B



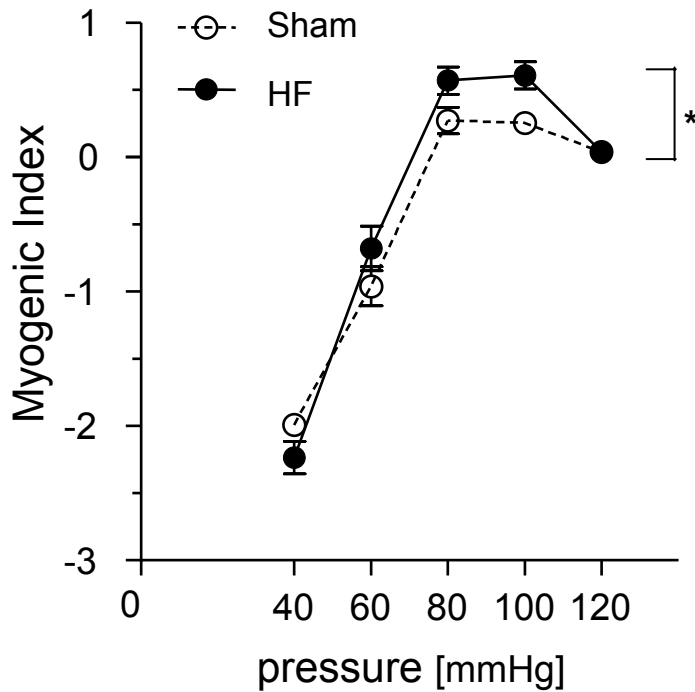
**Online Figure III: Vasomotor response to acetylcholine and sodium nitroprusside.** Concentration-dependent vasodilation to **(A)** acetylcholine (ACh) and **(B)** sodium nitroprusside (SNP) in mesenteric arteries (MA) pre-constricted with PE (3 μM) was not altered by HF. For all groups, n=6; data are mean ± SE; *P*=NS for all comparisons.

# Online Figure IV.



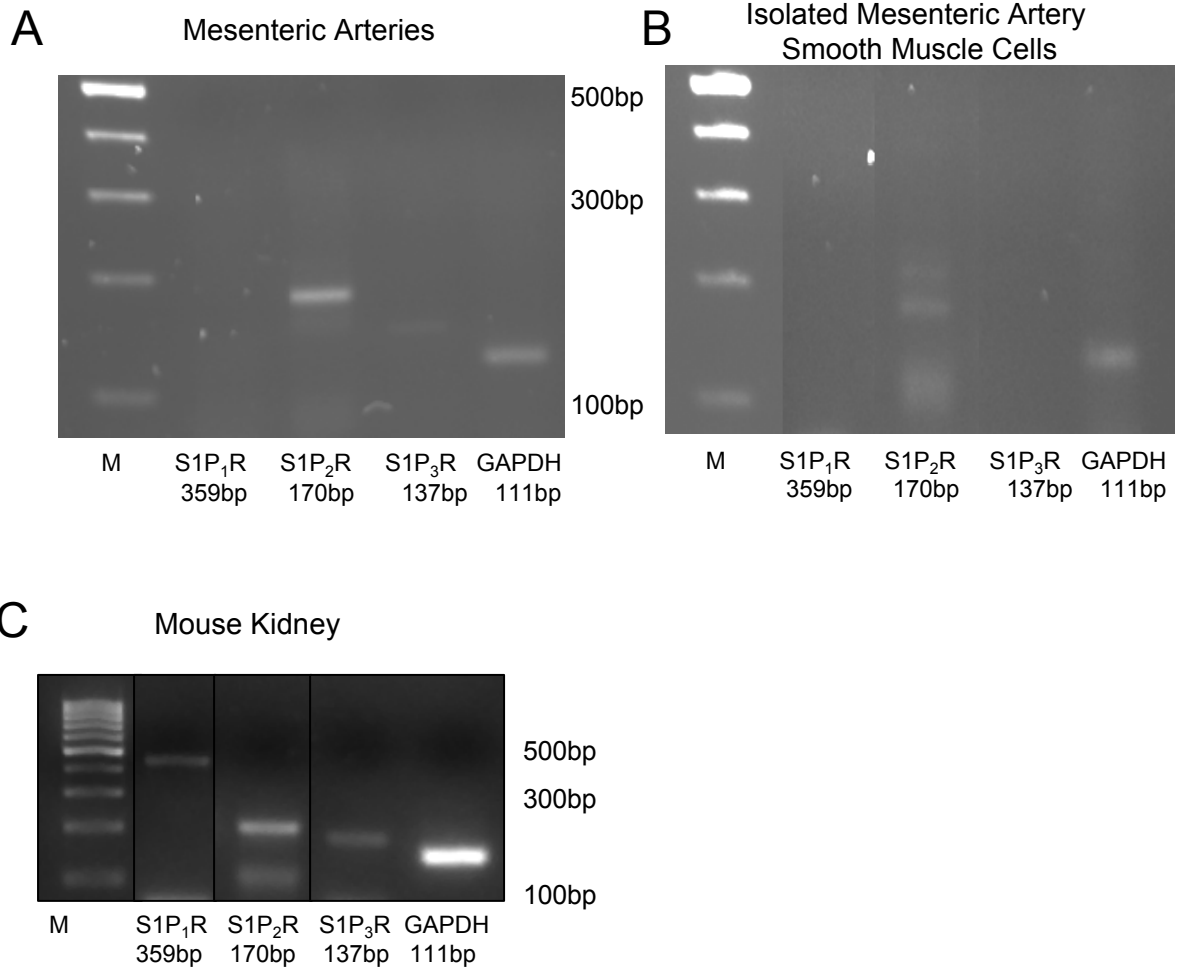
**Online Figure IV: Vasomotor response to Endothelin 1.** Concentration-dependent constriction responses to **(A)** Endothelin (ET-1) and **(B)** ET-1 after incubation with JTE-013 in mesenteric arteries (MA) pre-constricted with PE (3 μM). ET-1-induced vasoconstriction was increased in HF (\* $P < 0.05$  by 2 way ANOVA), but did not differ in sham vessels incubated with the S1P2 receptor antagonist JTE-013 ( $P = \text{NS}$ ). For all groups,  $n = 6$ ; Data are mean  $\pm$  SE.

## Online Figure V.



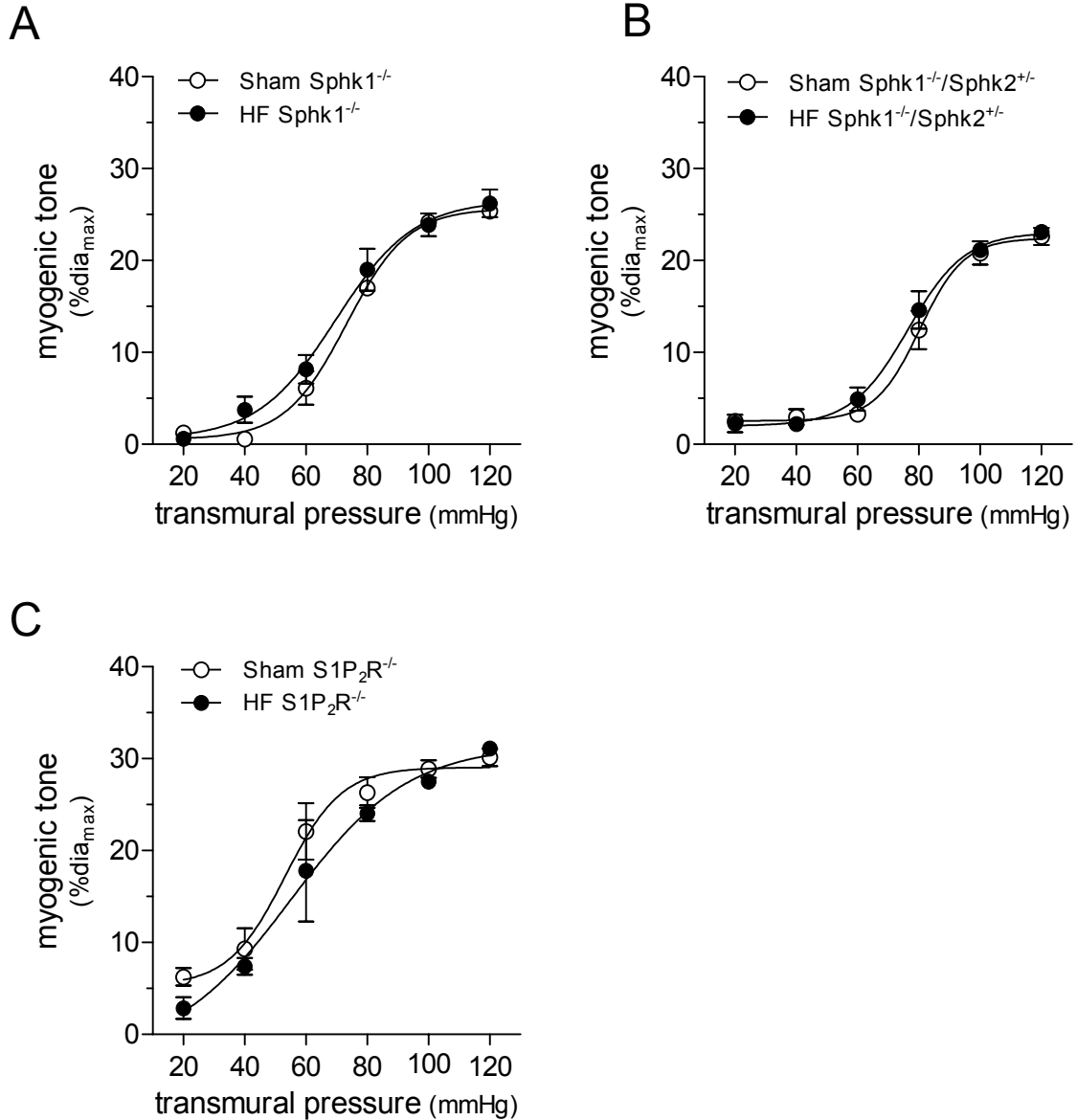
**Online Figure V: Myogenic index is increased in HF.** Myogenic index (MyoIndx) was augmented in mesenteric arteries (MA) isolated from HF vs. sham mice at 6 wk post-op; \* $P=0.015$  by 2-way ANOVA. MyoIndx was calculated as  $= 100 \times [(\Delta D/D_i)/\Delta p]$  where  $D_i$  is initial diameter before the change in intraluminal pressure;  $\Delta D$  is the change in diameter in response to the pressure change; and  $\Delta p$  is the magnitude of the applied change in pressure. For all groups,  $n=10$ ; Data are mean  $\pm$  SE.

# Online Figure VI.



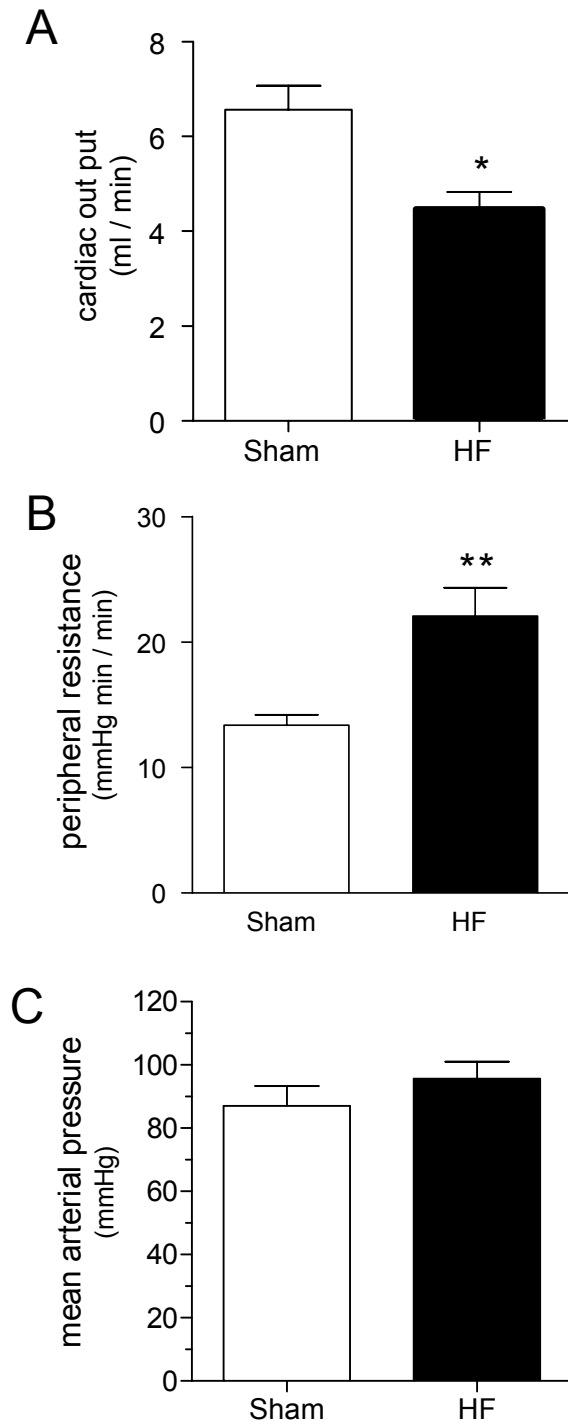
**Online Figure VI: Expression of S1P receptors in mesenteric arteries.** S1P<sub>1-3</sub> receptor mRNA expression in mouse mesenteric arteries (MA) (**A**) and vascular smooth muscle cells (VSMC) isolated from mouse MA (**B**). As a positive control, S1P<sub>1-3</sub> receptor expression was documented in mouse kidney (**C**) which is known to express all three S1P receptors.

# Online Figure VII.



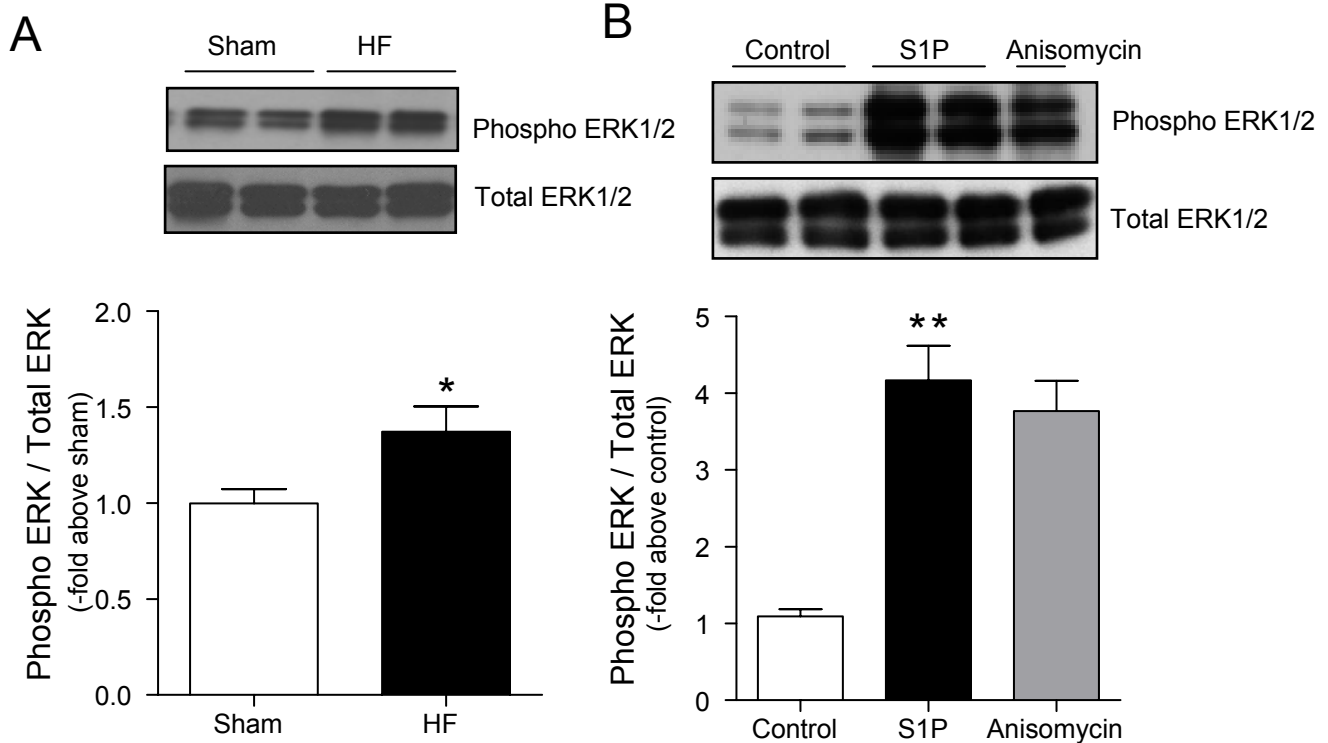
**Online Figure VII: Myogenic tone in mesenteric arteries from *Sphk1*<sup>-/-</sup>, *Sphk1*<sup>-/-</sup>/*Sphk2*<sup>+/-</sup>, and *S1P*<sub>2</sub>*R*<sup>-/-</sup> mice.** Myogenic responses (MR) in mesenteric arteries (MA) from *Sphk1*<sup>-/-</sup> (A), *Sphk1*<sup>-/-</sup>/*Sphk2*<sup>+/-</sup> (B), and *S1P*<sub>2</sub>*R*<sup>-/-</sup> (C) mice at 4 wk post surgery did not differ. For all groups, n=4; data are mean ± SE; P=NS for all comparisons.

## Online Figure VIII.



**Online Figure VIII: Hemodynamic parameters in *Sphk1<sup>-/-</sup>/Sphk2<sup>+/-</sup>* mice.** (A) cardiac output (CO), (B) peripheral resistance (PR) and (C) mean arterial pressure (MAP) at 4 wk post-op are shown in sham (n=5) and HF (n=6). In mice lacking *Sphk1* & heterozygous for *Sphk2*, CO was reduced and PR was increased in HF vs. sham. Data are mean  $\pm$  SE; \*  $P < 0.05$ ; \*\*  $P < 0.01$ ;  $P = \text{NS}$  for MAP.

# Online Figure IX.



**Online Figure IX: ERK1/2 levels in mesenteric arteries from HF and sham mice and S1P-dependent activation of ERK1/2 in mesenteric arteries from control mice.** Representative Western blots probed for total ERK1/2 and Thr202/Tyr204-phosphorylated ERK1/2 are shown for mesenteric artery (MA) protein extracts from **(A)** mice 6 wks post-MI (HF) or sham surgery (n=8-9), and **(B)** uninjured control MA treated with S1P (2  $\mu$ M for 10 min). Anisomycin (100 $\mu$ M) was used as positive control (n=3-5). Densitometric quantifications represent mean  $\pm$  SE; \* $P$ <0.05; \*\* $P$ <0.01.